DALTON

Linking and fragmentation of alkynes at a triruthenium centre

Kerry J. Adams, John J. Barker, Selby A. R. Knox* and A. Guy Orpen

School of Chemistry, University of Bristol, Bristol BS8 1TS, UK

The triruthenium μ_3-alkyne complex $[Ru_3(CO)_3(\mu\text{-}CO)(\mu_3\text{-}CO)\{\mu_3\text{-}C_2(CF_3)_2\}(\eta\text{-}C_5H_5)_2]$ **1** reacted with Me_3NO in MeCN to give $[Ru_3(MeCN)(CO)_2(\mu\text{-}CO)(\mu_3\text{-}CO)\{\mu_3\text{-}C_2(CF_3)_2\}(\eta\text{-}C_5H_5)_2]$ **2**. This with hexafluorobut-2-yne at or below room temperature gave $[Ru_3(CO)_2(\mu\text{-}CO)\{\mu_3\text{-}\eta^3\text{-}C_3(CF_3)_3\}(\mu_3\text{-}CCF_3)(\eta\text{-}C_5H_5)_2]$ **3**, shown by X-ray diffraction to contain a ruthenium triangle with μ_3-perfluoroethylidyne and $\mu_3\text{-}\eta^3\text{-}C_3(CF_3)_3$ ligands arising from cleavage of one of the hexafluorobut-2-yne molecules. In contrast, **2** reacted at room temperature with the alkynes diphenylethyne, methyl but-2-ynoate and but-2-yne to yield the species $[Ru_3(CO)_2(\mu\text{-}CO)_2\{\mu_3\text{-}C_4(CF_3)_2R(R')\}(\eta\text{-}C_5H_5)_2]$ (R = R′ = Ph; R = Me, R′ = CO_2Me; or R = R′ = Me) respectively. X-Ray diffraction studies on the first two of these showed that the alkynes have linked to form a $\mu_3\text{-}C_4(CF_3)_2R(R')$ ligand bound to a closed Ru_3 triangle *via* a doubly bridging interaction with one pair of metal atoms and an η^3-allyl mode with the other. Dimethyl acetylenedicarboxylate (dmad) reacted with **2** at room temperature differently again to give a structurally unidentified species $[Ru_3(CO)_5\{C_2(CF_3)_2\}\{C_2(CO_2Me)_2\}(\eta\text{-}C_5H_5)_2]$, which on heating afforded $[Ru_3(CO)_3\{\mu_3\text{-}C_4(CF_3)_2(CO_2Me)_2\}(\eta\text{-}C_5H_5)_2]$ **12**, revealed by X-ray diffraction to contain a *closo*-pentagonal-bipyramidal Ru_3C_4 cluster in which a $\mu_3\text{-}C_4(CF_3)_2(CO_2Me)_2$ ligand bridges an open ruthenium triangle. This complex was formed directly when **1** was heated with dmad in refluxing toluene. Analogous complexes $[Ru_3(CO)_3\{\mu_3\text{-}C_4(CF_3)_2R(R')\}(\eta\text{-}C_5H_5)_2]$ (R = Me, R′ = CO_2Me; R = R′ = Ph; or R = R′ = Me) were produced on heating **1** with methyl but-2-ynoate, diphenylethyne and but-2-yne respectively. The last two reactions also gave isomers $[Ru_3(CO)_3\{\mu_3\text{-}C_4(CF_3)R_2(CF_3)\}(\eta\text{-}C_5H_5)_2]$ (R = Ph or Me) in which formal insertion of the incoming alkyne into the co-ordinated $CF_3C{\equiv}CCF_3$ bond has occurred. In addition, the reaction of **1** with but-2-yne produced $[Ru_3(CO)_2(\mu\text{-}CO)\{\mu_3\text{-}\eta^3\text{-}C_3(CF_3)Me_2\}(\mu_3\text{-}CCF_3)(\eta\text{-}C_5H_5)_2]$ analogous to **3**. Diruthenium species $[Ru_2(CO)\{\mu\text{-}C_4(CF_3)_2R(R')\}(\eta\text{-}C_5H_5)_2]$ are formed in both toluene reflux reactions of **1** and room-temperature reactions of **2** as a result of triruthenium cluster degradation. Heating the room-temperature products $[Ru_3(CO)_2(\mu\text{-}CO)_2\{\mu_3\text{-}C_4(CF_3)_2R_2\}(\eta\text{-}C_5H_5)_2]$ confirms that these are intermediates in the formation of the complexes $[Ru_3(CO)_2(\mu\text{-}CO)\{\mu_3\text{-}\eta^3\text{-}C_3(CF_3)R_2\}(\mu_3\text{-}CCF_3)(\eta\text{-}C_5H_5)_2]$ and the isomeric *closo* clusters $[Ru_3(CO)_3\{\mu_3\text{-}C_4(CF_3)_2R_2\}(\eta\text{-}C_5H_5)_2]$ and $[Ru_3(CO)_3\{\mu_3\text{-}C_4(CF_3)R_2(CF_3)\}(\eta\text{-}C_5H_5)_2]$. Pathways for the processes leading to the various products are discussed.

The oligomerisation of alkynes at transition-metal centres has been well studied and proved a fertile area both for the synthesis of organic molecules, often otherwise inaccessible, and for gaining an insight into catalytic processes. Thus, for example, in this Laboratory the steps involved in the linking of up to four alkyne molecules at a dimolybdenum centre have been established,[1] suggesting how cyclooctatetraene may be formed in the Reppe process, while stepwise linking of up to four alkynes at a diruthenium centre has been shown to proceed differently.[2,3] Likewise, the long known but mechanistically obscure iron carbonyl-promoted linking of three ethyne molecules with CO to give cycloheptatrienone has been shown to occur stepwise at a diiron centre.[4]

We recently described the synthesis of a range of trinuclear μ_3-alkyne complexes $[Ru_2M(CO)_3(\mu\text{-}CO)(\mu_3\text{-}CO)(\mu_3\text{-}C_2R_2)(\eta\text{-}C_5H_5)_2]$ *via* the reactions of the unsaturated 32-electron complexes $[Ru_2(\mu\text{-}CO)(\mu\text{-}C_2R_2)(\eta\text{-}C_5H_5)_2]$ (R = Ph or CF_3) with $[M(CO)_4]$ (M = Fe or Ru) fragments.[5] These species were designed to provide an opportunity to extend our studies on alkyne oligomerisation and we describe here the results of an investigation based on the triruthenium hexafluorobut-2-yne complex $[Ru_3(CO)_3(\mu\text{-}CO)(\mu_3\text{-}CO)\{\mu_3\text{-}C_2(CF_3)_2\}(\eta\text{-}C_5H_5)_2]$ **1**, revealing new insights into the pathways for alkyne linking *and cleavage* at a trinuclear metal centre. The reactions of alkynes with trinuclear metal complexes, especially of the iron, ruthenium and osmium triad, have received considerable attention and been recently reviewed.[6]

Results and Discussion

The complex $[Ru_3(CO)_3(\mu\text{-}CO)(\mu_3\text{-}CO)\{\mu_3\text{-}C_2(CF_3)_2\}(\eta\text{-}C_5H_5)_2]$ **1** was found to be reactive towards alkynes when heated at reflux in toluene, with the results described below. However, experiments were also carried out with the acetonitrile derivative of **1**, the complex $[Ru_3(MeCN)(CO)_2(\mu\text{-}CO)(\mu_3\text{-}CO)\{\mu_3\text{-}C_2(CF_3)_2\}(\eta\text{-}C_5H_5)_2]$ **2**. The substitution lability of the acetonitrile ligand in the latter allowed reactions to be explored at room temperature, establishing the ease of alkyne linking and revealing the pathways involved. The results of these studies are described first.

Synthesis of $[Ru_3(MeCN)(CO)_2(\mu\text{-}CO)(\mu_3\text{-}CO)\{\mu_3\text{-}C_2(CF_3)_2\}(\eta\text{-}C_5H_5)_2]$ 2

Treatment of a dichloromethane solution of $[Ru_3(CO)_3(\mu\text{-}CO)(\mu_3\text{-}CO)\{\mu_3\text{-}C_2(CF_3)_2\}(\eta\text{-}C_5H_5)_2]$ **1** with 1 equivalent of trimethylamine oxide in acetonitrile resulted in the immediate and clean formation of $[Ru_3(MeCN)(CO)_2(\mu\text{-}CO)(\mu_3\text{-}CO)\{\mu_3\text{-}C_2(CF_3)_2\}(\eta\text{-}C_5H_5)_2]$ **2**, deduced from the IR spectrum. Complex **2** shows two terminal carbonyl bands at 2035 and 1984 cm^{-1}, a doubly bridging carbonyl at 1839 cm^{-1} and a triply bridging carbonyl at 1721 cm^{-1}. Evaporation of the reaction mixture yielded a dark red solid which was redissolved in dichloromethane prior to use. The likely structure of **2**, the reactions studied and the products isolated are illustrated in Scheme 1.

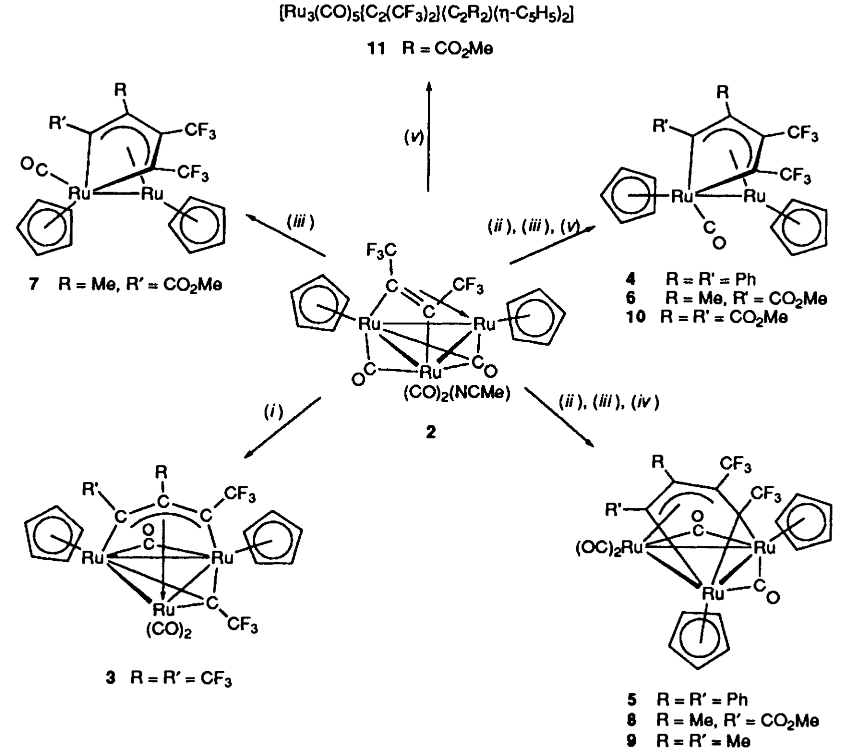

Scheme 1 Reactions of $[Ru_3(MeCN)(CO)_2(\mu\text{-}CO)(\mu_3\text{-}CO)\{\mu_3\text{-}C_2(CF_3)_2\}(\eta\text{-}C_5H_5)_2]$ **2** with alkynes at room temperature: (*i*) hexafluorobut-2-yne; (*ii*) diphenylethyne; (*iii*) methyl but-2-ynoate; (*iv*) but-2-yne; (*v*) dmad

Table 1 Analytical, physical and IR data for new complexes

Complex	M^a	Analysis (%)^{a,b} C	H	$\tilde{\nu}_{CO}{}^c/(cm^{-1})$
3	843 (843)	30.15 (29.95)	1.20 (1.20)	2053s, 2001m, 1836m
5	887 (887)	43.15 (43.40)	2.20 (2.30)	2043s, 1993m, 1849m, 1777w
6	622 (622)	38.55 (38.70)	2.55 (2.60)	1934s, 1720w, 1702w
7	622 (622)	38.75 (38.70)	2.55 (2.60)	2014s, 1713w
8	*d* (807)	33.65 (33.65)	1.95 (2.15)	2060s, 2053m, 2001w, 1855m, 1784m, 1706w
9	*d* (763)	34.65 (34.70)	2.15 (2.10)	2039s, 1989m, 1852m, 1777w
12	822 (822)	33.85 (33.65)	1.95 (1.95)^e	2060s, 1995m (br), 1750w, 1742w, 1713w
13	779 (779)	34.05 (34.00)	2.10 (2.05)	2057s, 1992m (br), 1716w
14b	859 (859)	43.45 (43.40)	2.35 (2.35)	2061s, 1999m, 1986w
15	702 (702)	49.80 (49.70)	2.80 (2.90)	1934s
16a	735 (735)	*d*		2050s, 1987m (br)
16b	735 (735)	*d*		2058s, 1995w, 1983w
17	735 (735)	*d*		2025s, 1965m, 1816m

[a] Calculated values in parentheses. [b] Samples recrystallised from dichloromethane–hexane unless otherwise stated. [c] Hexane solution. [d] Satisfactory values not obtained. [e] Sample recrystallised from dichloromethane–pentane.

Reactions of complex 2 with alkynes at room temperature

(*a*) **With hexafluorobut-2-yne.** Treatment of a dichloromethane solution of complex **2** with a two-fold excess of hexafluorobut-2-yne at room temperature for 18 h, followed by chromatography, afforded dark orange-brown $[Ru_3(CO)_2(\mu\text{-}CO)\{\mu_3\text{-}\eta^3\text{-}C_3(CF_3)_3\}(\mu_3\text{-}CCF_3)(\eta\text{-}C_5H_5)_2]$ **3** in 44% yield.

The IR spectrum of complex **3** in hexane shows two terminal carbonyl stretches at 2053 and 2001 cm^{-1} and a doubly bridging carbonyl band at 1836 cm^{-1}. A single resonance in the ^1H NMR spectrum at δ 5.41 for the cyclopentadienyl rings illustrates their equivalence, which is clearly shown also in the ^{13}C NMR spectra. Thus, the two outer carbons of the μ_3-allyl ligand are observed as a quartet (J_{CF} 38 Hz) at δ 173.9, with their associated CF_3 carbons as a single signal at δ 127.9 (q, J_{CF} 275 Hz). Two other resonances are seen at δ 133.0 and 122.0 (both quartets, J_{CF} 273 and 281 Hz respectively) for the central CF_3 group of the μ_3-allyl and the μ_3-CCF_3 group. A low-field quartet (J_{CF} 41 Hz) at δ 286.0 is characteristic of the μ_3-alkylidyne carbon. In the ^{19}F NMR spectrum the μ_3-CCF_3 group appears as a singlet at δ −48.0, the central CF_3 group of the allyl ligand as a broad unresolved multiplet at δ −46.5, and the two equivalent terminal allylic CF_3 groups as a quartet (J_{FF} 12 Hz) at δ −52.8. These data plus the mass spectroscopic and analytical data for **3** (Tables 1–3) are consistent with the structure shown in Scheme 1, which was confirmed by an X-ray diffraction study.

Molecular structure of complex **3**. The molecular structure of complex **3** was determined by X-ray diffraction and is shown in Fig. 1, with selected geometrical parameters listed in Table 4. As expected on the basis of NMR spectroscopy the molecule has approximate mirror symmetry. The three ruthenium atoms form a closed triangle with single Ru–Ru bond lengths Ru(1)–Ru(2) 2.718(1), Ru(1)–Ru(3) 2.716(1) and Ru(2)–Ru(3)

Table 2 Proton and ^{19}F NMR data for new complexes

Complex	^{1}H NMR (δ)[a]	^{19}F-{^{1}H} NMR (δ)[a]
3	5.41 (s, $\mathrm{2C_5H_5}$)	−46.5 (br, s, $\mathrm{CF_3}$), −48.0 (s, μ-$\mathrm{CCF_3}$), −52.8 (q, J_{FF} 12, $\mathrm{2CF_3}$)
5	7.64–6.51 (m, 10 H, 2Ph), 5.54 (s, 5 H, $\mathrm{C_5H_5}$), 4.88 (s, 5 H, $\mathrm{C_5H_5}$)[b]	−50.9 (q, J_{FF} 12, $\mathrm{CF_3}$), −52.0 (q, J_{FF} 12, $\mathrm{CF_3}$)
6	5.00 (s, 5 H, $\mathrm{C_5H_5}$), 4.96 (s, 5 H, $\mathrm{C_5H_5}$), 3.71 (s, 3 H, $\mathrm{CO_2Me}$), 2.14 (q, J_{HF} 2, 3 H, Me)	−49.6 (q, J_{FF} 12, $\mathrm{CF_3}$), −51.7 (q, J_{FF} 12, $\mathrm{CF_3}$)
7	5.21 (s, 5 H, $\mathrm{C_5H_5}$), 4.96 (s, 5 H, $\mathrm{C_5H_5}$), 3.75 (s, 3 H, $\mathrm{CO_2Me}$), 2.09 (q, J_{HF} 2, 3 H, Me)	−50.1 (q, J_{FF} 12, $\mathrm{CF_3}$), −51.1 (q, J_{FF} 12, $\mathrm{CF_3}$)
8	5.44 (br, s, 5 H, $\mathrm{C_5H_5}$), 5.20 (s, 5 H, $\mathrm{C_5H_5}$), 3.89 (s, 3 H, $\mathrm{CO_2Me}$), 2.27 (br, s, 3 H, Me)	−52.5 (br, m, $\mathrm{CF_3}$), −54.6 (m, $\mathrm{CF_3}$)
9	5.42 (s, 5 H, $\mathrm{C_5H_5}$), 5.26 (s, 5 H, $\mathrm{C_5H_5}$), 3.03 (s, 3 H, Me), 2.24 (s, 3 H, Me)	−52.5 (q, J_{FF} 10, $\mathrm{CF_3}$), −54.8 (q, J_{FF} 10, $\mathrm{CF_3}$)
12	4.91 (s, 10 H, $\mathrm{2C_5H_5}$), 3.90 (s, 3 H, Me), 3.47 (s, 3 H, Me)	−43.4 (br, unres. q, $\mathrm{CF_3}$), −49.1 (q, J_{FF} 12, $\mathrm{CF_3}$)
13	4.69 (s, 10 H, $\mathrm{2C_5H_5}$), 3.54 (s, 3 H, $\mathrm{CO_2Me}$), 2.81 (q, J_{HF} 2, 3 H, Me)	−42.8 (q, J_{FF} 12, $\mathrm{CF_3}$), −50.1 (q, J_{FF} 12, $\mathrm{CF_3}$)
14b	7.50–7.11 (m, 10 H, 2Ph), 4.80 (s, 10 H, $\mathrm{2C_5H_5}$)	−40.7 (s, $\mathrm{2CF_3}$)
15	7.25–6.56 (m, 10 H, 2Ph), 5.26 (s, 5 H, $\mathrm{C_5H_5}$), 5.16 (s, 5 H, $\mathrm{C_5H_5}$)	−50.0 (s, $\mathrm{2CF_3}$)
16a	4.53 (s, 10 H, $\mathrm{2C_5H_5}$), 2.80 (q, J_{HF} 2, 3 H, Me), 2.10 (s, 3 H, Me)	−42.5 (q, J_{FF} 13, $\mathrm{CF_3}$), −48.0 (qq, J_{FF} 13, J_{FH} 2, $\mathrm{CF_3}$)
16b	4.49 (s, 10 H, $\mathrm{2C_5H_5}$), 3.03 (q, J_{HF} 1, 6 H, 2Me)	−44.2 (unres. q, J_{FH} 1, $\mathrm{2CF_3}$)
17	5.28 (s, 5 H, $\mathrm{C_5H_5}$), 5.25 (s, 5 H, $\mathrm{C_5H_5}$), 2.74 (s, 3 H, Me), 2.45 (q, J_{HF} 2, 3 H, Me)	−47.3 (s, μ_3-$\mathrm{CCF_3}$), −48.6 (q, J_{FH} 2, $\mathrm{CF_3}$)

[a] In $\mathrm{CDCl_3}$ solution; coupling constants, *J*, in Hz. [b] In $\mathrm{CD_2Cl_2}$ solution.

Table 3 Carbon-13 NMR data for new complexes

Complex	^{13}C-{^{1}H} NMR (δ)[a]
3	286.0 (q, J_{CF} 41, μ_3-*C*$\mathrm{CF_3}$), 227.6 (s, μ-CO), 193.4 (s, 2CO), 173.9 (q, J_{CF} 38, 2*C*$\mathrm{CF_3}$), 133.0 (q, J_{CF} 273, $\mathrm{CF_3}$), 127.9 (q, J_{CF} 275, $\mathrm{2CF_3}$), 122.0 (q, J_{CF} 281, $\mathrm{CF_3}$), 92.5 (s, $\mathrm{2C_5H_5}$)[b]
5	244.2 (s, μ-CO), 219.6 (s, μ-CO), 197.4 (s, CO), 190.5 (s, CO), 142.4 (q, J_{CF} 35, *C*$\mathrm{CF_3}$), 152.1 (s), 134.6 (s), 132.7 (s), 130.7 (s), 128.4 (s), 128.0 (s), 127.8 (s), 127.4 (s), 126.3 (s), 126.2 (s), 126.1 (s) (2Ph), 124.8 (s, *C*Ph), 95.3 (s, $\mathrm{C_5H_5}$), 94.2 (s, $\mathrm{C_5H_5}$)[b]
6	198.8 (s, CO), 175.9 (s, *C*$\mathrm{O_2Me}$), 146.9 (s, *C*$\mathrm{CO_2Me}$), 138.5 (q, J_{CF} 42, *C*$\mathrm{CF_3}$), 124.5 (q, J_{CF} 278, $\mathrm{CF_3}$), 128.7 (q, J_{CF} 270, $\mathrm{CF_3}$), 110.6 (s, *C*Me), 104.1 (q, J_{CF} 35, *C*$\mathrm{CF_3}$), 86.8 (s, $\mathrm{C_5H_5}$), 85.6 (s, $\mathrm{C_5H_5}$), 52.0 (s, $\mathrm{CO_2}$*Me*), 19.3 (q, J_{CF} 2.5, Me)
7	199.8 (s, CO), 174.7 (s, *C*$\mathrm{O_2Me}$), 146.8 (s, *C*$\mathrm{CO_2Me}$), 139.6 (q, J_{CF} 41, *C*$\mathrm{CF_3}$), 128.0, (q, J_{CF} 269, $\mathrm{CF_3}$), 124.5 (q, J_{CF} 276, $\mathrm{CF_3}$), 102.5 (s, *C*Me), 96.1 (q, J_{CF} 40, *C*$\mathrm{CF_3}$), 85.5 (s, $\mathrm{C_5H_5}$), 81.2 (s, $\mathrm{C_5H_5}$), 50.8 (s, $\mathrm{CO_2}$*Me*), 18.6 (q, J_{CF} 4, Me)
8	94.4 (br, s, $\mathrm{C_5H_5}$), 92.8 (s, $\mathrm{C_5H_5}$)[b]
9	245.7 (s, μ-CO), 219.2 (s, μ-CO), 197.4 (s, CO), 187.1 (s, CO), 140.8 (q, J_{CF} 34, *C*$\mathrm{CF_3}$), 132.2 (q, J_{CF} 277, $\mathrm{CF_3}$), 124.3 (q, J_{CF} 276, $\mathrm{CF_3}$), 118.6 (s, *C*Me), 94.3 (s, $\mathrm{C_5H_5}$), 92.3 (s, $\mathrm{C_5H_5}$), 35.8 (s, Me), 15.2 (s, Me)[b]
12	197.3 (s, 3CO), 173.5 (s, *C*$\mathrm{O_2Me}$), 167.7 (s, *C*$\mathrm{O_2Me}$), 127.0 (q, J_{CF} 281, $\mathrm{CF_3}$), 125.0 (q, J_{CF} 275, $\mathrm{CF_3}$), 118.0 (s, *C*$\mathrm{CO_2Me}$), 99.5 (q, J_{CF} 46, *C*$\mathrm{CF_3}$), 77.0 (s, $\mathrm{2C_5H_5}$), 54.0 (s, Me), 52.2 (s, Me)
13	197.9 (s, 3CO), 174.3 (s, *C*$\mathrm{O_2Me}$), 127.4 (q, J_{CF} 271, $\mathrm{CF_3}$), 125.9 (q, J_{CF} 273, $\mathrm{CF_3}$), 123.1 (s, *C*$\mathrm{CO_2Me}$), 75.9 (s, $\mathrm{2C_5H_5}$), 52.2 (s, $\mathrm{CO_2}$*Me*), 22.7 (q, J_{CF} 4, Me)[b]
14b	198.1 (s, 3CO), 137.8 (s, 2*C*Ph), 134.8 (s), 127.8 (s), 127.0 (s) (2Ph), 128.6 (q, J_{CF} 274, $\mathrm{2CF_3}$), 112.9 (q, J_{CF} 42, 2*C*$\mathrm{CF_3}$), 76.4 (s, $\mathrm{2C_5H_5}$)[c]
15	199.0 (s, CO), 142.9 (q, J_{CF} 39, 2*C*$\mathrm{CF_3}$), 136.3 (s), 131.6 (s), 130.9 (s), 127.4 (s), 127.3 (s) (2Ph), 129.8 (q, J_{CF} 272, $\mathrm{2CF_3}$), 123.8 (s, 2*C*Ph), 87.2 (s, $\mathrm{C_5H_5}$), 84.8 (s, $\mathrm{C_5H_5}$)[c]
16a	199.2 (s, 3CO), 132.2 (s, *C*Me), 127.6 (q, J_{CF} 272, $\mathrm{CF_3}$), 126.4 (q, J_{CF} 275, $\mathrm{CF_3}$), 74.6 (s, $\mathrm{2C_5H_5}$), 17.0 (s, Me), 14.1 (s, Me)[b]
16b	199.9 (s, 3CO), 128.7 (q, J_{CF} 273, $\mathrm{2CF_3}$), 111.6 (q, J_{CF} 41, 2*C*$\mathrm{CF_3}$), 111.1 (s, 2*C*Me), 74.6 (s, $\mathrm{2C_5H_5}$), 16.4 (q, J_{CF} 4, 2Me)
17	277.6 (q, J_{CF} 42, μ_3-*C*$\mathrm{CF_3}$), 234.0 (s, μ-CO), 198.3 (s, CO), 197.3 (s, CO), 196.7 (s, *C*Me), 173.6 (q, J_{CF} 34, *C*$\mathrm{CF_3}$), 135.7 (s, *C*Me), 133.8 (q, J_{CF} 272, $\mathrm{CF_3}$), 129.8 (q, J_{CF} 276, $\mathrm{CF_3}$), 92.4 (s, $\mathrm{C_5H_5}$), 91.1 (s, $\mathrm{C_5H_5}$), 29.7 (s, Me), 19.4 (s, Me)

[a] In $\mathrm{CDCl_3}$ solution; coupling constants, *J*, in Hz. [b] Other signals not observed. [c] In $\mathrm{CD_2Cl_2}$ solution.

2.676(1) Å, consistent with a cluster valence electron count of 48. The most striking aspects of the molecule concern the binding of the organic ligands to the cluster. The μ_3-$\mathrm{C_3(CF_3)_3}$ unit is σ-bound to ruthenium atoms which carry η-$\mathrm{C_5H_5}$ ligands [Ru(2)–C(6) 2.074(5) and Ru(3)–C(8) 2.077(5) Å] and π-bound to the $\mathrm{Ru(CO)_3}$ unit [mean Ru(1)–C($\mathrm{CF_3}$) distance 2.211 Å]. On the opposite face of the $\mathrm{Ru_3}$ triangle is a slightly asymmetrically bound μ_3-$\mathrm{CCF_3}$ unit with Ru(1)–C(4) 1.975(5), Ru(2)–C(4) 2.014(5) and Ru(3)–C(4) 2.019(5) Å. The μ-CO ligand bridging the Ru(2)–Ru(3) edge lies 49.8° out of the $\mathrm{Ru_3}$ plane and is symmetrically bound.

Complex **3** clearly arises from a formal C≡C bond-scission process. Alkyne-scission reactions at trinuclear metal centres are not uncommon (see, for example, refs. 7–9) and hexafluorobut-2-yne cleavage has been reported.[10] However, the ease of the cleavage involved in the formation of **3** is unprecedented. Not only does it occur at room temperature, but below (see later).

***(b)* With diphenylethyne.** A dark red dichloromethane solution of complex **2** gradually turned green after stirring at room temperature for 20 h with 2 equivalents of diphenylethyne. Chromatography yielded two products: green $[\mathrm{Ru_3(CO)_2(\mu\text{-}CO)_2\{\mu_3\text{-}C_4(CF_3)_2Ph_2\}(\eta\text{-}C_5H_5)_2}]$ **5** in 38% yield and the known purple $[\mathrm{Ru_2(CO)\{\mu\text{-}C_4(CF_3)_2Ph_2\}(\eta\text{-}C_5H_5)_2}]$ **4**[2,3,11] in 11% yield. The latter is a typical 'ruthenole' product of alkyne coupling at a diruthenium centre and presumably arises here as a result of degradation of the triruthenium precursor.

The IR spectrum of complex **5** shows two terminal carbonyl bands at 2043 and 1993 cm^{-1} and bridging carbonyl absorptions at 1849 and 1777 cm^{-1}. The ^{1}H NMR spectrum shows the expected multiplet in the phenyl region between δ 7.64 and 6.51 and signals for inequivalent cyclopentadienyl groups at δ 5.54 and 4.88. The cyclopentadienyl carbons resonate at δ 95.3 and 94.2 in the ^{13}C NMR spectrum and the carbonyl carbon atoms are clearly seen at δ 244.2, 219.6, 197.4 and 190.5, but the $\mathrm{CF_3}$ carbons are obscured by the more intense peaks in the phenyl region. A quartet at δ 142.4 (J_{CF} 35 Hz) is assigned to one of the *C*$\mathrm{CF_3}$ carbons. The ^{19}F NMR spectrum reveals the presence of two $\mathrm{CF_3}$ groups in a quartet at δ −50.9 (J_{FF} 12 Hz) and a broad unresolved quartet at δ −52.0, the latter showing the effect of restricted rotation. The spectroscopic and analytical data were

Table 4 Selected bond lengths (Å) and angles (°) for complex **3**

Ru(1)–Ru(2)	2.718(1)	Ru(1)–Ru(3)	2.716(1)	Ru(1)–C(1)	1.905(5)
Ru(1)–C(2)	1.913(6)	Ru(1)–C(4)	1.975(5)	Ru(1)–C(6)	2.159(4)
Ru(1)–C(7)	2.318(5)	Ru(1)–C(8)	2.157(4)	Ru(2)–Ru(3)	2.676(1)
Ru(2)–C(3)	2.040(5)	Ru(2)–C(4)	2.014(5)	Ru(2)–C(6)	2.074(5)
Ru(2)–C(21)	2.218(9)	Ru(2)–C(22)	2.251(9)	Ru(2)–C(23)	2.237(6)
Ru(2)–C(24)	2.280(8)	Ru(2)–C(25)	2.230(8)	Ru(3)–C(3)	2.020(5)
Ru(3)–C(4)	2.019(5)	Ru(3)–C(8)	2.077(5)	Ru(3)–C(31)	2.229(6)
Ru(3)–C(32)	2.231(5)	Ru(3)–C(33)	2.246(6)	Ru(3)–C(34)	2.262(5)
Ru(3)–C(35)	2.240(5)	C(1)–O(1)	1.135(7)	C(2)–O(2)	1.133(7)
C(3)–O(3)	1.169(6)	C(4)–C(5)	1.507(8)	C(5)–F(5a)	1.350(7)
C(5)–F(5b)	1.339(6)	C(5)–F(5c)	1.335(7)	C(6)–C(7)	1.432(7)
C(6)–C(9)	1.513(6)	C(7)–C(8)	1.440(5)	C(7)–C(10)	1.517(8)
C(8)–C(11)	1.526(7)	C(9)–F(9a)	1.364(7)	C(9)–F(9b)	1.351(7)
C(9)–F(9c)	1.333(7)	C(10)–F(10a)	1.339(6)	C(10)–F(10b)	1.336(6)
C(10)–F(10c)	1.328(6)	C(11)–F(11a)	1.332(7)	C(11)–F(11b)	1.343(6)
C(11)–F(11c)	1.343(6)	C(21)–C(22)	1.415(11)	C(21)–C(25)	1.419(12)
C(22)–C(23)	1.438(15)	C(23)–C(24)	1.355(12)	C(24)–C(25)	1.383(11)
C(31)–C(32)	1.451(11)	C(31)–C(35)	1.396(10)	C(32)–C(33)	1.411(10)
C(33)–C(34)	1.392(9)	C(34)–C(35)	1.400(8)		

Ru(2)–Ru(1)–Ru(3)	59.0(1)	Ru(1)–Ru(2)–Ru(3)	60.5(1)	Ru(2)–C(6)–C(7)	124.2(3)	Ru(1)–C(6)–C(9)	122.4(3)
Ru(1)–Ru(3)–Ru(2)	60.5(1)	Ru(1)–C(1)–O(1)	177.1(6)	Ru(2)–C(6)–C(9)	116.1(4)	C(7)–C(6)–C(9)	119.2(4)
Ru(1)–C(2)–O(2)	178.5(5)	Ru(2)–C(3)–Ru(3)	82.4(2)	Ru(1)–C(7)–C(6)	65.4(2)	Ru(1)–C(7)–C(8)	65.2(2)
Ru(2)–C(3)–O(3)	138.2(4)	Ru(3)–C(3)–O(3)	139.0(4)	C(6)–C(7)–C(8)	114.8(4)	Ru(1)–C(7)–C(10)	143.8(3)
Ru(1)–C(4)–Ru(2)	85.9(2)	Ru(1)–C(4)–Ru(3)	85.7(2)	C(6)–C(7)–C(10)	122.9(4)	C(8)–C(7)–C(10)	122.2(4)
Ru(2)–C(4)–Ru(3)	83.1(2)	Ru(1)–C(4)–C(5)	125.0(3)	Ru(1)–C(8)–Ru(3)	79.8(2)	Ru(1)–C(8)–C(7)	77.4(2)
Ru(2)–C(4)–C(5)	131.1(4)	Ru(3)–C(4)–C(5)	130.3(3)	Ru(3)–C(8)–C(7)	123.4(3)	Ru(1)–C(8)–C(11)	121.8(3)
Ru(1)–C(6)–Ru(2)	79.9(2)	Ru(1)–C(6)–C(7)	77.5(3)	Ru(3)–C(8)–C(11)	116.8(3)	C(7)–C(8)–C(11)	119.2(4)

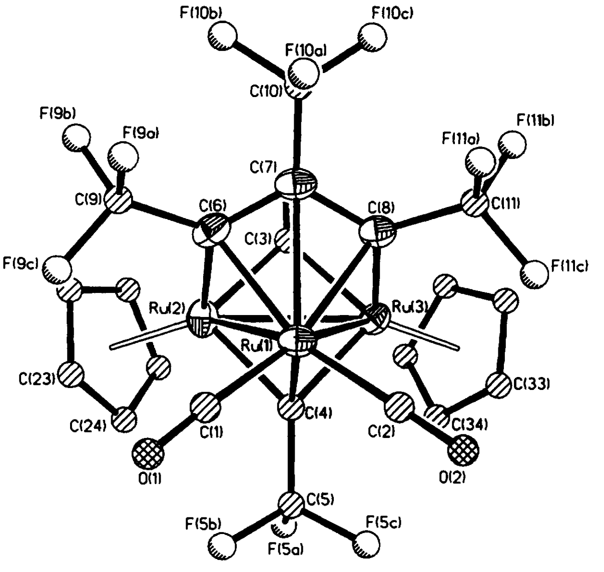

Fig. 1 Molecular structure of complex **3** showing the labelling scheme; all hydrogen atoms have been omitted for clarity

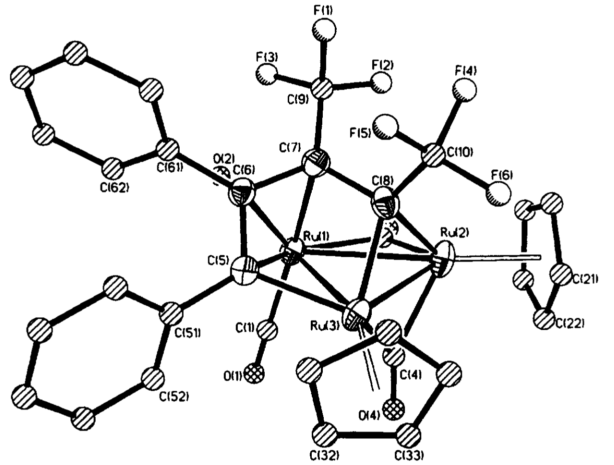

Fig. 2 Molecular structure of one of the two independent molecules of complex **5** showing the labelling scheme; all hydrogen atoms have been omitted for clarity

insufficient to characterise the complex fully and an X-ray diffraction study was therefore undertaken.

Molecular structure of complex **5**. The molecular structure of complex **5** is shown in Fig. 2 and important bond lengths and angles are given in Table 5. As expected the structure is asymmetric. There are two unique molecules in the crystal structure, which have near identical geometries. The molecular dimensions below refer to the illustrated molecule (Fig. 2) except where noted. As expected on the basis of the 48 cluster valence electrons, **5** contains a closed triruthenium triangle. The two alkynes have linked to form a μ_3-$C_4(CF_3)_2Ph_2$ ligand which is bonded to the Ru_3 unit *via* a μ-alkylidene function which bridges the two ruthenium atoms carrying η-C_5H_5 ligands [Ru(2)–C(8) 2.130(3), Ru(3)–C(8) 2.069(3) Å] and an η^3 interaction with the $Ru(CO)_3$ moiety [Ru(1)–C(5) 2.195(3), Ru(1)–C(6) 2.215(3) and Ru(1)–C(7) 2.191(3) Å]. The mean plane of the five-membered C_4Ru metallacycle incorporating Ru(3) is inclined at an angle of 48° to the Ru_3 plane. The reason for the large difference in the stretching frequencies of the bridging carbonyl ligands is apparently related to the different sites of the two μ-carbonyl ligands. One [C(3)] lies close to the plane of the metal triangle and the other [C(4)] near perpendicular to this plane, with consequent small differences in the C–O bond lengths [mean values C(3)–O(3) 1.165(4), C(4)–O(4) 1.179(4) Å].

An intriguing feature of the structure of complex **5** is the relatively long C(7)–C(8) bond length of 1.519(5) Å, which may be compared with the allylic C(6)–C(7) and C(5)–C(6) bond lengths of 1.442(4) and 1.433(4) Å respectively. The C(7)–C(8) bond was originally the triple bond of the hexafluorobut-2-yne and it is attractive to conclude that a complex analogous to **5** is initially formed in the reaction of **2** with this alkyne and that it is this bond which cleaves in a rearrangement to give **3**. The NMR data obtained during a low-temperature reaction of **2** with hexafluorobut-2-yne (see below) are consistent with this suggestion.

Table 5 Selected bond lengths (Å) and angles (°) for complex **5**

Ru(1)–C(2)	1.884(4)	Ru(1)–C(1)	1.911(4)	Ru(1)–C(3)	2.152(3)	Ru(1)–C(7)	2.191(3)
Ru(1)–C(5)	2.195(3)	Ru(1)–C(6)	2.215(3)	Ru(1)–Ru(2)	2.823(1)	Ru(1)–Ru(3)	2.823(1)
Ru(2)–C(3)	2.010(4)	Ru(2)–C(4)	2.029(4)	Ru(2)–C(8)	2.130(3)	Ru(2)–C(21)	2.212(5)
Ru(2)–C(24)	2.240(5)	Ru(2)–C(23)	2.247(4)	Ru(2)–C(22)	2.249(5)	Ru(2)–C(25)	2.258(5)
Ru(2)–Ru(3)	2.674(1)	Ru(3)–C(4)	2.043(4)	Ru(3)–C(8)	2.069(3)	Ru(3)–C(5)	2.087(3)
Ru(3)–C(31)	2.243(4)	Ru(3)–C(35)	2.260(4)	Ru(3)–C(34)	2.267(4)	Ru(3)–C(32)	2.273(4)
Ru(3)–C(33)	2.286(4)	C(1)–O(1)	1.143(5)	C(2)–O(2)	1.143(4)	C(3)–O(3)	1.165(4)
C(4)–O(4)	1.179(4)	C(5)–C(6)	1.433(4)	C(5)–C(51)	1.500(4)	C(51)–C(52)	1.390(5)
C(51)–C(56)	1.401(5)	C(52)–C(53)	1.385(6)	C(53)–C(54)	1.363(8)	C(54)–C(55)	1.382(8)
C(55)–C(56)	1.391(6)	C(6)–C(7)	1.442(4)	C(6)–C(61)	1.506(4)	C(61)–C(62)	1.390(5)
C(61)–C(66)	1.396(5)	C(62)–C(63)	1.386(5)	C(63)–C(64)	1.377(6)	C(64)–C(65)	1.381(7)
C(65)–C(66)	1.391(5)	C(7)–C(9)	1.510(5)	C(7)–C(8)	1.519(5)	C(9)–F(2)	1.343(4)
C(9)–F(1)	1.349(4)	C(9)–F(3)	1.350(5)	C(8)–C(10)	1.514(5)	C(10)–F(6)	1.343(5)
C(10)–F(4)	1.363(5)	C(10)–F(5)	1.363(4)	C(21)–C(22)	1.353(9)	C(21)–C(25)	1.388(9)
C(22)–C(23)	1.355(8)	C(23)–C(24)	1.416(9)	C(24)–C(25)	1.436(8)	C(31)–C(35)	1.391(7)
C(31)–C(32)	1.415(7)	C(32)–C(33)	1.392(7)	C(33)–C(34)	1.409(6)	C(34)–C(35)	1.404(6)
Ru(1a)–C(1a)	1.891(4)	Ru(1a)–C(2a)	1.916(4)	Ru(1a)–C(3a)	2.124(4)	Ru(1a)–C(7a)	2.182(3)
Ru(1a)–C(5a)	2.193(3)	Ru(1a)–C(6a)	2.226(3)	Ru(1a)–Ru(3a)	2.794(1)	Ru(1a)–Ru(2a)	2.833(1)
Ru(2a)–C(4a)	2.018(4)	Ru(2a)–C(3a)	2.036(4)	Ru(2a)–C(8a)	2.119(3)	Ru(2a)–C(24a)	2.228(5)
Ru(2a)–C(21a)	2.239(5)	Ru(2a)–C(23a)	2.242(4)	Ru(2a)–C(22a)	2.251(4)	Ru(2a)–C(25a)	2.264(5)
Ru(2a)–Ru(3a)	2.675(1)	Ru(3a)–C(8a)	2.064(3)	Ru(3a)–C(4a)	2.067(4)	Ru(3a)–C(5a)	2.094(3)
Ru(3a)–C(34a)	2.234(4)	Ru(3a)–C(35a)	2.242(4)	Ru(3a)–C(31a)	2.253(5)	Ru(3a)–C(33a)	2.258(4)
Ru(3a)–C(32a)	2.268(5)	C(1a)–O(1a)	1.136(5)	C(2a)–O(2a)	1.144(5)	C(3a)–O(3a)	1.161(4)
C(4a)–O(4a)	1.178(5)	C(5a)–C(6a)	1.434(4)	C(5a)–C(51a)	1.500(4)	C(51a)–C(52a)	1.391(5)
C(51a)–C(56a)	1.398(5)	C(52a)–C(53a)	1.388(6)	C(53a)–C(54a)	1.370(7)	C(54a)–C(55a)	1.380(6)
C(55a)–C(56a)	1.381(5)	C(6a)–C(7a)	1.439(4)	C(6a)–C(61a)	1.500(4)	C(61a)–C(62a)	1.393(5)
C(61a)–C(66a)	1.392(5)	C(62a)–C(63a)	1.400(5)	C(63a)–C(64a)	1.377(7)	C(64a)–C(65a)	1.375(7)
C(65a)–C(66a)	1.391(5)	C(7a)–C(8a)	1.516(4)	C(7a)–C(9a)	1.522(5)	C(9a)–F(3a)	1.345(4)
C(9a)–F(2a)	1.349(5)	C(9a)–F(1a)	1.350(5)	C(8a)–C(10a)	1.518(5)	C(10a)–F(6a)	1.346(5)
C(10a)–F(4a)	1.352(5)	C(10a)–F(5a)	1.357(5)	C(21a)–C(25a)	1.401(8)	C(21a)–C(22a)	1.411(8)
C(22a)–C(23a)	1.380(7)	C(23a)–C(24a)	1.396(9)	C(24a)–C(25a)	1.413(9)	C(31a)–C(35a)	1.348(8)
C(31a)–C(32a)	1.386(10)	C(32a)–C(33a)	1.406(9)	C(33a)–C(34a)	1.397(8)	C(34a)–C(35a)	1.345(7)
Ru(2)–Ru(1)–Ru(3)	56.54(2)	Ru(3)–Ru(2)–Ru(1)	61.74(3)	Ru(3a)–Ru(2a)–Ru(1a)	60.90(2)	Ru(2a)–Ru(3a)–Ru(1a)	62.34(2)
Ru(2)–Ru(3)–Ru(1)	61.72(3)	O(1)–C(1)–Ru(1)	176.9(4)	O(1a)–C(1a)–Ru(1a)	178.6(4)	O(2a)–C(2a)–Ru(1a)	178.5(4)
O(2)–C(2)–Ru(1)	178.1(4)	O(3)–C(3)–Ru(2)	140.3(3)	O(3a)–C(3a)–Ru(2a)	138.6(3)	O(3a)–C(3a)–Ru(1a)	135.6(4)
O(3)–C(3)–Ru(1)	134.2(3)	Ru(2)–C(3)–Ru(1)	85.33(13)	Ru(2a)–C(3a)–Ru(1a)	85.79(13)	O(4a)–C(4a)–Ru(2a)	138.8(3)
O(4)–C(4)–Ru(2)	138.2(3)	O(4)–C(4)–Ru(3)	139.1(3)	O(4a)–C(4a)–Ru(3a)	138.7(3)	Ru(2a)–C(4a)–Ru(3a)	81.8(2)
Ru(2)–C(4)–Ru(3)	82.10(14)	C(6)–C(5)–C(51)	120.6(3)	C(6a)–C(5a)–C(51a)	118.2(3)	C(6a)–C(5a)–Ru(3a)	116.1(2)
C(6)–C(5)–Ru(3)	115.1(2)	C(51)–C(5)–Ru(3)	122.0(2)	C(51a)–C(5a)–Ru(3a)	122.7(2)	C(6a)–C(5a)–Ru(1a)	72.3(2)
C(6)–C(5)–Ru(1)	71.8(2)	C(51)–C(5)–Ru(1)	129.1(2)	C(51a)–C(5a)–Ru(1a)	131.7(2)	Ru(3a)–C(5a)–Ru(1a)	81.34(11)
Ru(3)–C(5)–Ru(1)	82.44(11)	C(5)–C(6)–C(7)	112.3(3)	C(5a)–C(6a)–C(7a)	111.1(3)	C(5a)–C(6a)–C(61a)	121.9(3)
C(5)–C(6)–C(61)	121.6(3)	C(7)–C(6)–C(61)	126.1(3)	C(7a)–C(6a)–C(61a)	127.0(3)	C(5a)–C(6a)–Ru(1a)	69.8(2)
C(5)–C(6)–Ru(1)	70.3(2)	C(7)–C(6)–Ru(1)	70.0(2)	C(7a)–C(6a)–Ru(1a)	69.3(2)	C(61a)–C(6a)–Ru(1a)	127.1(2)
C(61)–C(6)–Ru(1)	126.8(2)	C(6)–C(7)–C(9)	120.1(3)	C(6a)–C(7a)–C(8a)	115.7(3)	C(6a)–C(7a)–C(9a)	120.2(3)
C(6)–C(7)–C(8)	116.2(3)	C(9)–C(7)–C(8)	121.5(3)	C(8a)–C(7a)–C(9a)	121.2(3)	C(6a)–C(7a)–Ru(1a)	72.6(2)
C(6)–C(7)–Ru(1)	71.8(2)	C(9)–C(7)–Ru(1)	119.3(2)	C(8a)–C(7a)–Ru(1a)	92.5(2)	C(9a)–C(7a)–Ru(1a)	119.7(2)
C(8)–C(7)–Ru(1)	92.0(2)	C(10)–C(8)–C(7)	113.5(3)	C(7a)–C(8a)–C(10a)	113.8(3)	C(7a)–C(8a)–Ru(3a)	109.9(2)
C(10)–C(8)–Ru(3)	118.2(3)	C(7)–C(8)–Ru(3)	109.4(2)	C(10a)–C(8a)–Ru(3a)	117.9(3)	C(7a)–C(8a)–Ru(2a)	111.8(2)
C(10)–C(8)–Ru(2)	118.7(2)	C(7)–C(8)–Ru(2)	113.5(2)	C(10a)–C(8a)–Ru(2a)	119.5(2)	Ru(3a)–C(8a)–Ru(2a)	79.48(12)
Ru(3)–C(8)–Ru(2)	79.09(12)	Ru(3a)–Ru(1a)–Ru(2a)	56.76(3)				

(*c*) **With methyl but-2-ynoate.** Methyl but-2-ynoate (MeC≡CCO$_2$Me) reacted slowly with a dichloromethane solution of complex **2** at room temperature to form three major products after 24 h, readily separated by chromatography. The first to be eluted was identified as *trans*-[Ru$_2$(CO){μ-C$_4$(CF$_3$)$_2$Me(CO$_2$Me)}(η-C$_5$H$_5$)$_2$] **6**, isolated in 10% yield as a pink solid. The second, produced in 13% yield, was isomeric yellow *cis*-[Ru$_2$(CO){μ-C$_4$(CF$_3$)$_2$Me(CO$_2$Me)}(η-C$_5$H$_5$)$_2$] **7**. These dinuclear complexes were fully characterised by physical and spectroscopic methods (Tables 1–3) and comparison with similar known complexes.[2,3,11] The third product, produced in 15% yield, was identified spectroscopically (Tables 1–3) and by X-ray diffraction as [Ru$_3$(CO)$_2$(μ-CO)$_2${μ$_3$-C$_4$(CF$_3$)$_2$Me(CO$_2$Me)}(η-C$_5$H$_5$)$_2$] **8**, analogous to **5** (see below).

The IR spectrum of complex **8** shows five metal carbonyl stretching bands instead of the expected four, at 2060, 2053, 2001, 1855 and 1784 cm^{-1}, in addition to the C=O stretch of the CO$_2$Me group at 1706 cm^{-1}. This probably indicates the presence of isomers in solution, interconverting on the NMR time-scale, in that the ^{1}H NMR spectrum shows two cyclopentadienyl ring signals, one broad at δ 5.44 and one sharp at δ 5.20, while a broad resonance is also seen for the alkynic methyl group, at δ 2.27, and a sharp signal at δ 3.89 for the CO$_2$Me methyl group. A high-temperature ^{1}H NMR study showed sharpening of the broad peaks as the temperature was increased from 25 to 90 °C. The ^{19}F NMR spectrum of **8** shows two broad unresolved multiplets at δ −52.5 and −54.6 for the CF$_3$ groups, consistent with their restricted rotation.

Molecular structure of complex **8**. The molecular structure of complex **8** (Fig. 3 and Table 6) is very similar to that of **5** and reveals that the two alkynes have combined in a manner which minimises steric crowding, with the C (methyl) carbon of methyl but-2-ynoate linked with hexafluorobut-2-yne. As in complex **5**, the five-membered metallacycle formed by the two alkyne molecules and Ru(3) is inclined by 48° to the triruthenium plane. The elongation of the former hexafluorobut-2-yne triple bond [C(7)–C(8) 1.508(4) Å] compared with the allylic C–C bond lengths [C(6)–C(7) 1.433(4) and C(5)–C(6) 1.422(4)] is again notable.

Table 6 Selected bond lengths (Å) and angles (°) for complex **8**

Ru(1)–C(1)	1.883(3)	Ru(1)–C(2)	1.919(3)	Ru(1)–C(3)	2.091(3)	Ru(1)–C(5)	2.145(2)
Ru(1)–C(7)	2.184(3)	Ru(1)–C(6)	2.240(3)	Ru(1)–Ru(3)	2.7959(5)	Ru(1)–Ru(2)	2.8217(4)
Ru(2)–C(4)	2.002(3)	Ru(2)–C(3)	2.070(3)	Ru(2)–C(8)	2.099(3)	Ru(2)–C(21)	2.206(3)
Ru(2)–C(24)	2.226(3)	Ru(2)–C(23)	2.247(3)	Ru(2)–C(25)	2.248(3)	Ru(2)–C(22)	2.251(3)
Ru(2)–Ru(3)	2.6709(5)	Ru(3)–C(4)	2.054(3)	Ru(3)–C(5)	2.060(3)	Ru(3)–C(8)	2.069(2)
Ru(3)–C(35)	2.215(3)	Ru(3)–C(34)	2.245(3)	Ru(3)–C(31)	2.253(3)	Ru(3)–C(33)	2.264(3)
Ru(3)–C(32)	2.297(3)	C(1)–O(1)	1.134(3)	C(2)–O(2)	1.129(4)	C(3)–O(3)	1.160(3)
C(4)–O(4)	1.174(3)	C(5)–C(6)	1.422(4)	C(5)–C(9)	1.500(4)	C(6)–C(7)	1.433(4)
C(6)–C(11)	1.506(4)	C(7)–C(12)	1.507(4)	C(7)–C(8)	1.508(4)	C(8)–C(13)	1.508(4)
C(9)–O(6)	1.194(3)	C(9)–O(5)	1.334(3)	O(5)–C(10)	1.449(4)	C(12)–F(12b)	1.331(4)
C(12)–F(12c)	1.342(4)	C(12)–F(12a)	1.344(4)	C(13)–F(13a)	1.343(3)	C(13)–F(13b)	1.350(4)
C(13)–F(13c)	1.351(3)	C(21)–C(25)	1.399(5)	C(21)–C(22)	1.407(5)	C(22)–C(23)	1.391(5)
C(23)–C(24)	1.429(6)	C(24)–C(25)	1.384(5)	C(31)–C(32)	1.362(5)	C(31)–C(35)	1.400(6)
C(32)–C(33)	1.392(5)	C(33)–C(34)	1.392(5)	C(34)–C(35)	1.385(5)		
Ru(3)–Ru(1)–Ru(2)	56.8(2)	Ru(3)–Ru(2)–Ru(1)	61.3(2)	C(5)–C(6)–C(11)	124.0(3)	C(7)–C(6)–C(11)	125.9(3)
Ru(2)–Ru(3)–Ru(1)	62.10(2)	O(1)–C(1)–Ru(1)	178.1(3)	C(5)–C(6)–Ru(1)	67.50(14)	C(7)–C(6)–Ru(1)	69.0(2)
O(2)–C(2)–Ru(1)	177.4(3)	O(3)–C(3)–Ru(2)	136.5(2)	C(11)–C(6)–Ru(1)	127.8(2)	C(6)–C(7)–C(12)	120.3(2)
O(3)–C(3)–Ru(1)	138.1(2)	Ru(2)–C(3)–Ru(1)	85.40(10)	C(6)–C(7)–C(8)	115.7(2)	C(12)–C(7)–C(8)	120.9(2)
O(4)–C(4)–Ru(2)	139.8(2)	O(4)–C(4)–Ru(3)	137.2(2)	C(6)–C(7)–Ru(1)	73.3(2)	C(12)–C(7)–Ru(1)	119.3(2)
Ru(2)–C(4)–Ru(3)	82.37(10)	C(6)–C(5)–C(9)	120.3(2)	C(8)–C(7)–Ru(1)	92.9(2)	C(13)–C(8)–C(7)	113.6(2)
C(6)–C(5)–Ru(3)	117.1(2)	C(9)–C(5)–Ru(3)	120.8(2)	C(13)–C(8)–Ru(3)	116.6(2)	C(7)–C(8)–Ru(3)	109.2(2)
C(6)–C(5)–Ru(1)	74.8(2)	C(9)–C(5)–Ru(1)	124.4(2)	C(13)–C(8)–Ru(2)	121.2(2)	C(7)–C(8)–Ru(2)	111.9(2)
Ru(3)–C(5)–Ru(1)	83.32(9)	C(5)–C(6)–C(7)	110.0(2)	Ru(3)–C(8)–Ru(2)	79.69(9)		

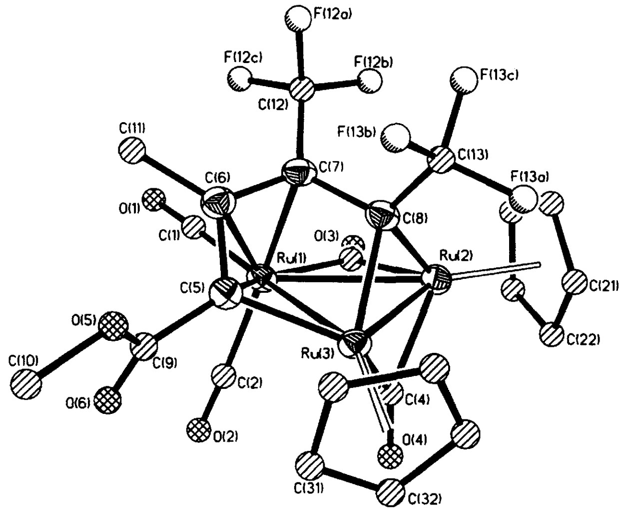

Fig. 3 Molecular structure of complex **8** showing the labelling scheme; all hydrogen atoms have been omitted for clarity

(*d*) **With but-2-yne.** Reaction of complex **2** with but-2-yne at room temperature over 16 h resulted in the formation of green crystalline $[Ru_3(CO)_2(\mu\text{-}CO)_2\{\mu_3\text{-}C_4(CF_3)_2Me_2\}(\eta\text{-}C_5H_5)_2]$ **9** in 22% yield after chromatography. This was identified by physical and spectroscopic methods (Tables 1–3) and is clearly analogous to complexes **5** and **8**. No diruthenium products were formed in this reaction.

(*e*) **With dimethyl acetylenedicarboxylate (dmad).** The room-temperature reaction of complex **2** with dmad ($MeO_2CC{\equiv}C\text{-}CO_2Me$) gave two products. One was identified spectroscopically as the known[2,3,11] diruthenium complex *trans*-$[Ru_2(CO)\{\mu\text{-}C_4(CF_3)_2(CO_2Me)_2\}(\eta\text{-}C_5H_5)_2]$ **10**, produced in 42% yield. The other, yellow microcrystalline, product had a mass spectrum and elemental analyses consistent with an empirical formula $[Ru_3(CO)_5\{C_2(CF_3)_2\}\{C_2(CO_2Me)_2\}(\eta\text{-}C_5H_5)_2]$ **11**, but the IR and NMR spectra were very complicated, indicating the existence of several isomers and preventing full characterisation. The apparent presence of five CO ligands in **11**, *cf.* four in the precursor **2**, implies a scavenging of CO in solution. Recrystallisation of **11** from several different solvent systems resulted in formation of clumps of yellow needle-shaped crystals, but these proved unsuitable for X-ray diffraction study.

Whether or not the two alkyne molecules in complex **11** are linked remains uncertain but heating the complex in toluene led to a new species $[Ru_3(CO)_3\{\mu_3\text{-}C_4(CF_3)_2(CO_2Me)_2\}(\eta\text{-}C_5H_5)_2]$ **12** in 53% yield, described fully in the next section.

Reactions of complex 1 with alkynes in toluene at reflux

The reactions of the pentacarbonyl complex **1**, the parent of **2**, with alkynes in refluxing toluene gave the products summarised in Scheme 2.

(*a*) **With dimethyl acetylenedicarboxylate.** The reaction of complex **1** with dmad in refluxing toluene for 3 h gave three products, two of which were the same as in the room-temperature reaction of **2** with dmad, namely the complexes **10** (25%) and **11** (18%). The third product was identified as the novel *closo*-pentagonal-bipyramidal cluster complex $[Ru_3(CO)_3\{\mu_3\text{-}C_4(CF_3)_2(CO_2Me)_2\}(\eta\text{-}C_5H_5)_2]$ **12**, isolated in 22% yield, also formed by heating **11**.

The IR spectrum of complex **12** shows a strong, sharp carbonyl band at 2060 cm^{-1} and a medium-intensity broad band at 1995 cm^{-1}, indicative of the presence of an $Ru(CO)_3$ unit. The ^1H NMR spectrum shows a single resonance for the cyclopentadienyl rings at δ 4.91, indicating their equivalence, but the CO_2Me methyl groups are inequivalent, resonating at δ 3.47 and 3.90. The three terminal carbonyls show one signal in the ^{13}C NMR spectrum at δ 197.3, consistent with the usual rapid rotation of such a unit, and peaks at δ 173.5 and 167.7 for the CO_2Me carbon atoms. The CF_3 groups are also inequivalent, seen as two quartets at δ 127.0 and 125.0, with J_{CF} 281 and 275 Hz respectively. As in the ^1H NMR spectrum, the cyclopentadienyl resonance is upfield of typical values, at δ 77.0. The ^{19}F NMR spectrum of **12** shows a broad signal at δ −43.4, probably due to restricted rotation, and a quartet at δ −49.1 (J_{FF} 12 Hz). The NMR, mass spectroscopic and analytical data proved insufficient unequivocally to establish the structure, prompting an X-ray diffraction study.

Molecular structure of complex **12**. The structure of complex **12** is shown in Fig. 4 and important bond lengths and angles are listed in Table 7. There are two independent molecules in the crystal structure with very similar geometries. In the following

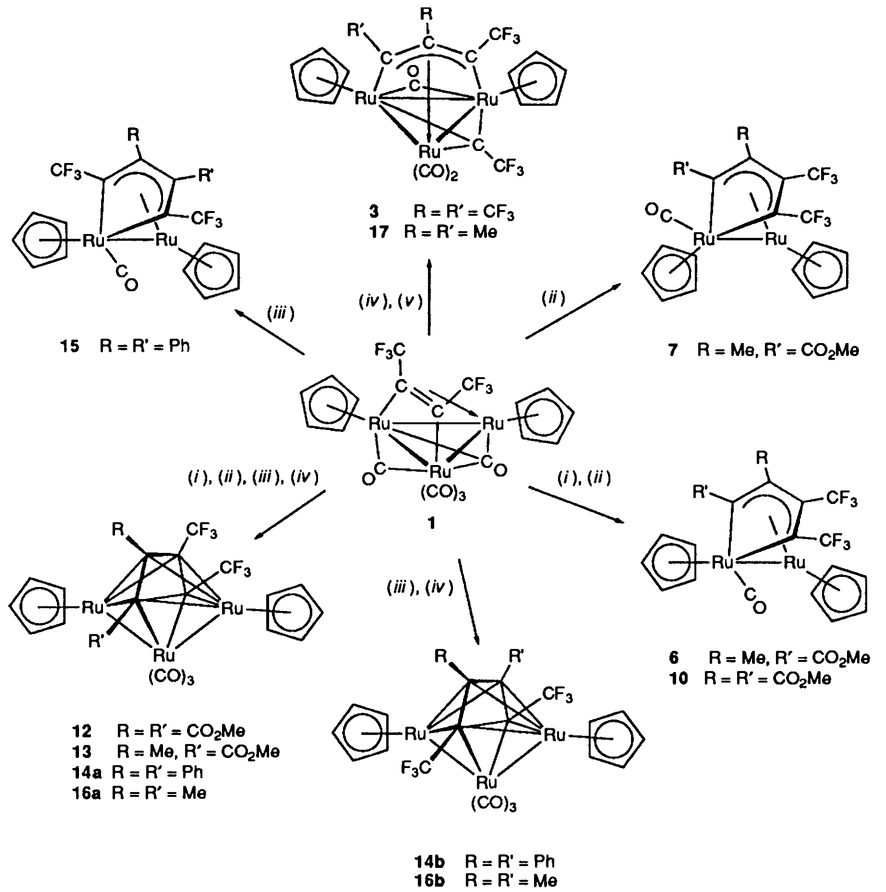

Scheme 2 Reactions of $[Ru_3(CO)_3(\mu\text{-}CO)(\mu_3\text{-}CO)\{\mu_3\text{-}C_2(CF_3)_2\}(\eta\text{-}C_5H_5)_2]$ **1** with alkynes in toluene at reflux: (*i*) dmad; (*ii*) methyl but-2-ynoate; (*iii*) diphenylethyne; (*iv*) but-2-yne; (*v*) hexafluorobut-2-yne

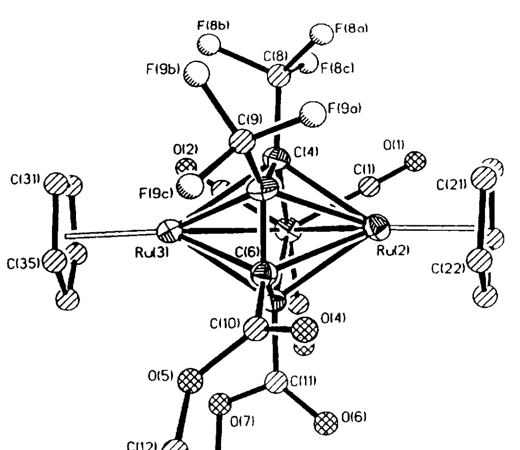

Fig. 4 Molecular structure of one of the two independent molecules of complex **12** showing the labelling scheme; all hydrogen atoms have been omitted for clarity

discussion the molecular dimensions refer to the molecule illustrated in Fig. 4.

The three metal atoms form an open triangle, with the ruthenium atoms carrying $\eta\text{-}C_5H_5$ ligands non-bonded [Ru(2) ··· Ru(3) 3.559 Å] and Ru(1)–Ru(2) and Ru(1)–Ru(3) at typical single-bond distances of 2.704(1) and 2.705(1) Å respectively. The two alkynes have linked to form a C_4R_4 unit which is σ,σ'-bound to Ru(1), creating a metallacyclopentadienyl ring [Ru(1)–C(4) 2.158(3), Ru(1)–C(7) 2.121(4) Å], and π-bound to Ru(2) and Ru(3). The bridging organic ligand is positioned centrally between the two non-bonded ruthenium atoms, giving the molecule a mirror plane. The cyclopentadienyl rings are approximately parallel to the central C_4Ru plane, with angles between them and the central plane of 5.0 and 7.8°, thus giving a 'sandwich' conformation. The CO_2Me side chains are twisted from each other, the angle between the two CO_2Me planes being 47.8°.

Complex **12** is four electrons short of obeying the 18-electron rule overall, having 46 cluster valence electrons, but is best classified by polyhedral skeletal electron pair (PSEP) theory, according to which it is a *closo*-pentagonal bipyramidal Ru_3C_4 cluster with eight such pairs. It can also be considered, less rigorously, as a 'triple-decker sandwich' analogous to species such as $[(\eta\text{-}C_5R_5)Ru(C_5R_5)Ru(\eta\text{-}C_5R_5)]^+$, by invoking the isolobal relationship between an $Ru(CO)_3$ vertex and a CR^+ vertex.[12–14]

(*b*) **With methyl but-2-ynoate.** The reaction of complex **1** with methyl but-2-ynoate in refluxing toluene for 2.5 h gives a *closo* cluster complex $[Ru_3(CO)_3\{\mu_3\text{-}C_4(CF_3)_2(Me)(CO_2Me)\}(\eta\text{-}C_5H_5)_2]$ **13** in 17% yield, analogous to **12**. The spectroscopic and other data for **13** are very similar to those of **12** and are in Tables 1–3. The data do not indicate which 'end' of methyl but-2-ynoate has linked with the hexafluorobut-2-yne ligand of **1**, but in view of the nature of **6**–**8** it appears safe to assume that linking occurs preferentially with the C(Me) carbon. A 22% yield of the *cis* and *trans* isomers of $[Ru_2(CO)\{\mu\text{-}C_4(CF_3)_2Me(CO_2Me)\}(\eta\text{-}C_5H_5)_2]$ **6** and **7** is also obtained from the reaction, arising from triruthenium cluster degradation.

(*c*) **With diphenylethyne.** Refluxing a mixture of complex **1** and diphenylethyne in toluene for 1.5 h caused a change from red to dark orange and upon chromatography two bands were obtained. The first gave an orange microcrystalline solid,

Table 7 Selected bond lengths (Å) and angles for complex **12**

Ru(1)–Ru(2)	2.704(1)	Ru(1)–Ru(3)	2.705(1)	Ru(1)–C(1)	1.908(5)	Ru(1)–C(2)	1.918(4)
Ru(1)–C(3)	1.912(5)	Ru(1)–C(4)	2.158(3)	Ru(1)–C(7)	2.121(4)	Ru(2)–C(4)	2.213(3)
Ru(2)–C(5)	2.188(4)	Ru(2)–C(6)	2.177(4)	Ru(2)–C(7)	2.245(3)	Ru(2)–C(21)	2.161(4)
Ru(2)–C(22)	2.156(4)	Ru(2)–C(23)	2.169(5)	Ru(2)–C(24)	2.174(4)	Ru(2)–C(25)	2.170(4)
Ru(3)–C(4)	2.245(4)	Ru(3)–C(5)	2.166(3)	Ru(3)–C(6)	2.187(3)	Ru(3)–C(7)	2.211(3)
Ru(3)–C(31)	2.145(6)	Ru(3)–C(32)	2.145(5)	Ru(3)–C(33)	2.156(4)	Ru(3)–C(34)	2.152(5)
Ru(3)–C(35)	2.135(6)	C(1)–O(1)	1.134(6)	C(2)–O(2)	1.125(5)	C(3)–O(3)	1.133(6)
C(4)–C(8)	1.506(6)	C(4)–C(5)	1.474(6)	C(8)–F(8a)	1.339(4)	C(8)–F(8b)	1.343(5)
C(8)–F(8c)	1.319(6)	C(5)–C(9)	1.524(5)	C(5)–C(6)	1.483(5)	C(9)–F(9a)	1.315(4)
C(9)–F(9b)	1.333(5)	C(9)–F(9c)	1.345(7)	C(6)–C(10)	1.503(6)	C(6)–C(7)	1.453(5)
C(10)–O(4)	1.193(4)	C(10)–O(5)	1.336(5)	O(5)–C(12)	1.452(7)	C(7)–C(11)	1.503(6)
C(11)–O(6)	1.191(5)	C(11)–O(7)	1.331(4)	O(7)–C(13)	1.442(7)	C(21)–C(22)	1.413(9)
C(21)–C(25)	1.381(8)	C(22)–C(23)	1.412(8)	C(23)–C(24)	1.403(8)	C(24)–C(25)	1.408(7)
C(31)–C(32)	1.370(11)	C(31)–C(35)	1.417(14)	C(32)–C(33)	1.363(11)	C(33)–C(34)	1.331(10)
C(34)–C(35)	1.354(10)	Ru(1a)–Ru(2a)	2.706(1)	Ru(1a)–Ru(3a)	2.716(1)	Ru(1a)–C(1a)	1.901(5)
Ru(1a)–C(2a)	1.893(5)	Ru(1a)–C(3a)	1.914(3)	Ru(1a)–C(4a)	2.166(3)	Ru(1a)–C(7a)	2.124(4)
Ru(2a)–C(4a)	2.202(4)	Ru(2a)–C(5a)	2.176(3)	Ru(2a)–C(6a)	2.176(4)	Ru(2a)–C(7a)	2.241(3)
Ru(2a)–C(21a)	2.184(5)	Ru(2a)–C(22a)	2.172(6)	Ru(2a)–C(23a)	2.166(4)	Ru(2a)–C(24a)	2.175(4)
Ru(2a)–C(25a)	2.182(5)	Ru(3a)–C(4a)	2.263(4)	Ru(3a)–C(5a)	2.180(4)	Ru(3a)–C(6a)	2.192(4)
Ru(3a)–C(7a)	2.231(3)	Ru(3a)–C(31a)	2.181(4)	Ru(3a)–C(32a)	2.166(6)	Ru(3a)–C(33a)	2.166(5)
Ru(3a)–C(34a)	2.153(5)	Ru(3a)–C(35a)	2.164(5)	C(1a)–O(1a)	1.134(6)	C(2a)–O(2a)	1.144(7)
C(3a)–O(3a)	1.135(4)	C(4a)–C(8a)	1.511(5)	C(4a)–C(5a)	1.470(6)	C(8a)–F(8aa)	1.320(5)
C(8a)–F(8ab)	1.338(6)	C(8a)–F(8ac)	1.317(6)	C(5a)–C(9a)	1.519(4)	C(5a)–C(6a)	1.491(5)
C(9a)–F(9aa)	1.302(6)	C(9a)–F(9ab)	1.318(6)	C(9a)–F(9ac)	1.336(6)	C(6a)–C(10a)	1.506(6)
C(6a)–C(7a)	1.452(4)	C(10a)–O(4a)	1.191(6)	C(10a)–O(5a)	1.334(5)	O(5a)–C(12a)	1.453(8)
C(7a)–C(11a)	1.492(5)	C(11a)–O(6a)	1.201(6)	C(11a)–O(7a)	1.330(5)	O(7a)–C(13a)	1.451(4)
C(21a)–C(22a)	1.417(7)	C(21a)–C(25a)	1.412(8)	C(22a)–C(23a)	1.404(6)	C(23a)–C(24a)	1.401(8)
C(24a)–C(25a)	1.410(5)	C(31a)–C(32a)	1.402(8)	C(31a)–C(35a)	1.401(9)	C(32a)–C(33a)	1.408(6)
C(33a)–C(34a)	1.413(10)	C(34a)–C(35a)	1.406(7)				
Ru(2)–Ru(1)–Ru(3)	82.3(1)	Ru(1)–C(1)–O(1)	179.4(4)	Ru(2a)–Ru(1a)–Ru(3a)	82.2(1)	Ru(1a)–C(1a)–O(1a)	179.1(3)
Ru(1)–C(2)–O(2)	178.6(5)	Ru(1)–C(3)–O(3)	177.4(5)	Ru(1a)–C(2a)–O(2a)	177.6(4)	Ru(1a)–C(3a)–O(3a)	177.8(5)
Ru(1)–C(4)–Ru(2)	76.4(1)	Ru(1)–C(4)–Ru(3)	75.8(1)	Ru(1a)–C(4a)–Ru(2a)	76.6(1)	Ru(1a)–C(4a)–Ru(3a)	75.6(1)
Ru(2)–C(4)–Ru(3)	105.9(2)	Ru(1)–C(4)–C(8)	121.2(3)	Ru(2a)–C(4a)–Ru(3a)	106.0(1)	Ru(1a)–C(4a)–C(8a)	121.4(3)
Ru(2)–C(4)–C(8)	126.0(2)	Ru(3)–C(4)–C(8)	127.3(2)	Ru(2a)–C(4a)–C(8a)	125.4(3)	Ru(3a)–C(4a)–C(8a)	127.8(3)
Ru(1)–C(4)–C(5)	119.1(3)	Ru(2)–C(4)–C(5)	69.5(2)	Ru(1a)–C(4a)–C(5a)	119.0(2)	Ru(2a)–C(4a)–C(5a)	69.4(2)
Ru(3)–C(4)–C(5)	67.6(2)	C(8)–C(4)–C(5)	119.7(3)	Ru(3a)–C(4a)–C(5a)	67.7(2)	C(8a)–C(4a)–C(5a)	119.6(3)
Ru(2)–C(5)–Ru(3)	109.6(1)	Ru(2)–C(5)–C(4)	71.4(2)	Ru(2a)–C(5a)–Ru(3a)	109.9(1)	Ru(2a)–C(5a)–C(4a)	71.3(2)
Ru(3)–C(5)–C(4)	73.4(2)	Ru(2)–C(5)–C(9)	129.2(2)	Ru(3a)–C(5a)–C(4a)	73.8(2)	Ru(2a)–C(5a)–C(9a)	128.9(3)
Ru(3)–C(5)–C(9)	120.7(2)	C(4)–C(5)–C(9)	127.5(4)	Ru(3a)–C(5a)–C(9a)	120.8(3)	C(4a)–C(5a)–C(9a)	127.6(3)
Ru(2)–C(5)–C(6)	69.8(2)	Ru(3)–C(5)–C(6)	70.8(2)	Ru(2a)–C(5a)–C(6a)	70.0(2)	Ru(3a)–C(5a)–C(6a)	70.5(2)
C(4)–C(5)–C(6)	112.4(3)	C(9)–C(5)–C(6)	120.0(4)	C(4a)–C(5a)–C(6a)	112.4(3)	C(9a)–C(5a)–C(6a)	119.8(4)
Ru(2)–C(6)–Ru(3)	109.3(2)	Ru(2)–C(6)–C(5)	70.5(2)	Ru(2a)–C(6a)–Ru(3a)	109.4(2)	Ru(2a)–C(6a)–C(5a)	70.0(2)
Ru(3)–C(6)–C(5)	69.4(2)	Ru(2)–C(6)–C(10)	123.0(2)	Ru(3a)–C(6a)–C(5a)	69.6(2)	Ru(2a)–C(6a)–C(10a)	122.8(3)
Ru(3)–C(6)–C(10)	127.6(2)	C(5)–C(6)–C(10)	124.1(3)	Ru(3a)–C(6a)–C(10a)	127.7(3)	C(5a)–C(6a)–C(10a)	125.1(3)
Ru(2)–C(6)–C(7)	73.4(2)	Ru(3)–C(6)–C(7)	71.6(2)	Ru(2a)–C(6a)–C(7a)	73.3(2)	Ru(3a)–C(6a)–C(7a)	72.3(2)
C(5)–C(6)–C(7)	112.3(3)	C(10)–C(6)–C(7)	123.6(3)	C(5a)–C(6a)–C(7a)	112.4(3)	C(10a)–C(6a)–C(7a)	122.4(3)
Ru(1)–C(7)–Ru(2)	76.5(1)	Ru(1)–C(7)–Ru(3)	77.3(1)	Ru(1a)–C(7a)–Ru(2a)	76.6(1)	Ru(1a)–C(7a)–Ru(3a)	77.1(1)
Ru(2)–C(7)–Ru(3)	106.0(1)	Ru(1)–C(7)–C(6)	121.4(3)	Ru(2a)–C(7a)–Ru(3a)	105.8(1)	Ru(1a)–C(7a)–C(6a)	121.2(2)
Ru(2)–C(7)–C(6)	68.3(2)	Ru(3)–C(7)–C(6)	69.8(2)	Ru(2a)–C(7a)–C(6a)	68.4(2)	Ru(3a)–C(7a)–C(6a)	69.4(2)
Ru(1)–C(7)–C(11)	123.3(2)	Ru(2)–C(7)–C(11)	124.4(2)	Ru(1a)–C(7a)–C(11a)	123.3(2)	Ru(2a)–C(7a)–C(11a)	123.6(3)
Ru(3)–C(7)–C(11)	127.9(2)	C(6)–C(7)–C(11)	115.2(3)	Ru(3a)–C(7a)–C(11a)	129.0(3)	C(6a)–C(7a)–C(11a)	115.4(3)

shown to be a mixture of the isomeric *closo* clusters $[Ru_3(CO)_3\{\mu_3\text{-}C_4(CF_3)_2Ph_2\}(\eta\text{-}C_5H_5)_2]$ **14a** and $[Ru_3(CO)_3\{\mu_3\text{-}C_4(CF_3)Ph_2(CF_3)\}(\eta\text{-}C_5H_5)_2]$ **14b**. The dominance of **14b** allowed a pure sample to be obtained by chromatography, but no data other than the IR spectrum in the carbonyl stretching region (2057, 1999 and 1985 cm^{-1}) could be obtained for the minor isomer **14a**. The major isomer **14b** had similar stretches at 2061, 1999 and 1986 cm^{-1}. On the basis of NMR data (Tables 2 and 3) it is clear that **14b** contains the symmetrical $\mu\text{-}C(CF_3)CPhCPhC(CF_3)$ unit shown in Scheme 2, arising from formal insertion of diphenylethyne into the C≡C bond of hexafluorobut-2-yne. Thus, the CF_3 groups in the ^{13}C and ^{19}F NMR spectra are equivalent, being seen as a quartet at δ 112.9 (J_{CF} 42 Hz) and a singlet at δ −40.7 respectively. The mechanistic implications of this structure are discussed below. It is suggested that **14a** has the asymmetric structure shown, similar to **12** and **13**, arising from straightforward linking of diphenylethyne with hexafluorobut-2-yne. In support, the reaction of **1** with but-2-yne (following section) has been shown unequivocally to produce isomeric *closo* clusters **16a** and **16b** analogous to **14a** and **14b**.

The other major product from the reaction of complex **1** with diphenylethyne was the new dinuclear ruthenole complex *trans*-$[Ru_2(CO)\{\mu\text{-}C_4(CF_3)Ph_2(CF_3)\}(\eta\text{-}C_5H_5)_2]$ **15**, formed in 14% yield. This degradation product is again formally derived by insertion of diphenylethyne into the hexafluorobut-2-yne molecule and is isomeric with complex **4**, in which the alkynes have simply linked.

(*d*) **With but-2-yne.** The reaction of complex **1** with but-2-yne in refluxing toluene for 3 h gave three products. Like the reaction with diphenylethyne, two isomeric *closo* cluster complexes were formed, but these were now readily separated by chromatography, giving yellow $[Ru_3(CO)_3\{\mu_3\text{-}C_4(CF_3)_2Me_2\}(\eta\text{-}C_5H_5)_2]$ **16a** in 17% yield and orange $[Ru_3(CO)_3\{\mu_3\text{-}C_4(CF_3)Me_2(CF_3)\}(\eta\text{-}C_5H_5)_2]$ **16b** in 46% yield. Again, the isomer due to formal alkyne insertion into the C≡C bond of hexafluorobut-2-yne is the major form. Both isomers were

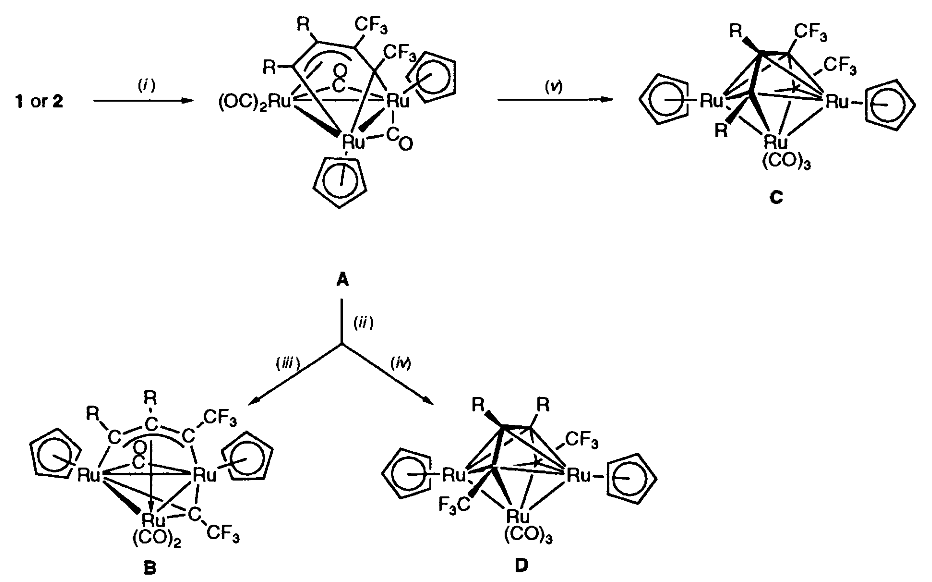

Scheme 3 Reaction pathways: (*i*) RC≡CR; (*ii*) heat, −CO, C–C bond cleavage; (*iii*) μ_3-CCF$_3$ formation; (*iv*) C–C bond regeneration; (*v*) heat, −CO, C–C bond retention

fully characterised spectroscopically (Tables 1–3) but satisfactory elemental analyses could not be obtained because of the presence of an impurity not separable by chromatography. This shows a single CO stretch in the IR spectrum at 1922 cm^{-1}, suggesting it is a dinuclear complex similar to those already described.

The third product of the reaction was dark orange $[Ru_3(CO)_2(\mu\text{-}CO)\{\mu_3\text{-}\eta^3\text{-}C_3(CF_3)Me_2\}(\mu_3\text{-}CCF_3)(\eta\text{-}C_5H_5)_2]$ **17**, isolated in 24% yield and clearly identified by IR and NMR spectra as an analogue of **3** (see Tables 1–3). Thus, for example, the ^{1}H NMR spectrum has two resonances at δ 5.28 and 5.25 assigned to the inequivalent cyclopentadienyl rings, a singlet at δ 2.74 due to the terminal allylic methyl group, and a quartet at δ 2.45 (J_{HF} 2 Hz) for the central allylic methyl coupled to the adjacent CF$_3$ group. In the ^{13}C NMR spectrum a characteristic low-field quartet (J_{CF} 42 Hz) at δ 277.6 is seen for the alkylidyne carbon of the μ_3-CCF$_3$ group, while the allylic *C*Me*C*Me*C*(CF$_3$) carbons are observed at δ 196.7(s), 135.7(s), and 173.6 (q, J_{CF} 34 Hz) respectively. In the ^{19}F NMR spectrum the μ_3-CCF$_3$ group is seen as a singlet signal at δ −47.3 and the allylic CF$_3$ group as a quartet at δ −48.6 (J_{FH} 2 Hz).

(*e*) **With hexafluorobut-2-yne.** The reaction of complex **1** with hexafluorobut-2-yne in toluene in a sealed tube for 4 h at 100 °C gave only complex **3**, in 49% yield, mirroring the room-temperature reaction of the acetonitrile derivative **2** with hexafluorobut-2-yne.

Reaction pathways

In attempting to rationalise the above observations the relationships between four types of complex needed to be established: the 'room temperature' species $[Ru_3(CO)_2(\mu\text{-}CO)_2\{\mu_3\text{-}C_4(CF_3)_2R_2\}(\eta\text{-}C_5H_5)_2]$ (type **A**), the μ_3-alkylidyne complexes $[Ru_3(CO)_2(\mu\text{-}CO)\{\mu_3\text{-}\eta^3\text{-}C_3(CF_3)R_2\}(\mu_3\text{-}CCF_3)(\eta\text{-}C_5H_5)_2]$ **B**, and the isomeric *closo* clusters $[Ru_3(CO)_3\{\mu_3\text{-}C_4(CF_3)_2R_2\}(\eta\text{-}C_5H_5)_2]$ **C** and $[Ru_3(CO)_3\{\mu_3\text{-}C_4(CF_3)R_2\text{-}(CF_3)\}(\eta\text{-}C_5H_5)_2]$ **D**. The diruthenium complexes formed are seen as degradation products arising from these four and are not considered further.

It is evident that the type **A** complexes **5**, **8** and **9** may represent the initial species formed when **1** or **2** reacts with an alkyne, acting as a precursor of types **B**–**D**. The reduction in the C≡C bond order of hexafluorobut-2-yne from three to one in the complexes **A** makes them particularly attractive as putative intermediates in the formation of **B** and **D**, which require cleavage of this bond. These expectations were confirmed by heating samples of the complexes.

Heating $[Ru_3(CO)_2(\mu\text{-}CO)_2\{\mu_3\text{-}C_4(CF_3)_2Ph_2\}(\eta\text{-}C_5H_5)_2]$ **5** in toluene at reflux for 1 h gave **14b** and **15** in 45 and 4% yields respectively, similar to those obtained when **1** is heated with diphenylethyne, but **14a** was not observed. Likewise, heating $[Ru_3(CO)_2(\mu\text{-}CO)_2\{\mu_3\text{-}C_4(CF_3)_2Me_2\}(\eta\text{-}C_5H_5)_2]$ **9** gave the complexes **16b** and **17**, but no **16a**. Heating $[Ru_3(CO)_2\text{-}(\mu\text{-}CO)_2\{\mu_3\text{-}C_4(CF_3)_2Me(CO_2Me)\}(\eta\text{-}C_5H_5)_2]$ **8** gave **6** and **13**, as for the direct reaction of **1** with but-2-ynoate.

The above observations establish the likely intermediacy of complexes of type **A** in the formation of **B** and **D**, and in the case of **8**, of **C**. All complexes of types **B**–**D** were shown to be thermally stable in refluxing toluene, ruling out any pathways involving these as intermediates in the formation of the others. The absence of a product of type **C** when **5** and **9** are heated therefore requires that a minor, unidentified pathway to such species exists when **1** is heated with an alkyne. Scheme 3 is proposed to account for the main results of the reactions of the complexes **1** and **2** with alkynes. This envisages that the initial complex formed is of type **A** in each case, which then undergoes CO loss to induce either: (*a*) rearrangement *without C–C bond cleavage* to give the asymmetric *closo* cluster species **C**, or (*b*) *C–C bond cleavage*, followed by the CCF$_3$ fragment either: (*i*) adopting the μ_3 mode to give an allyl/alkylidyne complex **B**, or (*ii*) linking with the other end of the allyl fragment to give a symmetric *closo* cluster complex of type **D**.

While PhC≡CPh apparently follows path (*b*)(*ii*), MeC≡CMe follows both (*b*)(*i*) and (*b*)(*ii*), whereas MeC≡CCO$_2$Me follows path (*a*) and it appears MeO$_2$CC≡CCO$_2$Me does also. The unidentified pentacarbonyl species isolated at room temperature from the reaction of complex **2** with the latter is suggested to be a precursor of a short-lived tetracarbonyl species **A**, formed on heating the pentacarbonyl, which gives the appropriate *closo* cluster **C**.

That the species **A** can be thermally very unstable and may also have a precursor was established through a low-temperature NMR study of the reaction of hexafluorobut-2-yne with complex **2**. This showed the formation of an initial product at −70 °C (equal-intensity cyclopentadienyl signals at δ 5.28 and 5.18), continuing to grow in at −50 °C and being joined at −40 °C by a new signal at δ 5.56 and a pair of equal-intensity signals at δ 5.24 and 5.19. This last group increased in relative intensity at −30 °C and at −20 °C the cyclopentadienyl

Table 8 Details of structure analyses for complexes **3**, **5**, **8** and **12**[a]

	3	**5**	**8**	**12**
Formula	$C_{21}H_{10}F_{12}O_3Ru_3$	$C_{32}H_{20}F_6O_4Ru_3$	$C_{23}H_{16}F_6O_6Ru_3$	$C_{23}H_{16}F_{16}O_7Ru_3$
M	841.5	885.69	805.57	821.6
Crystal system	Monoclinic	Triclinic	Triclinic	Triclinic
Space group (no.)	$P2_1/c$ (14)	$P\bar{1}$(2)	$P\bar{1}$(2)	$P\bar{1}$(2)
a/Å	16.746(4)	9.614(3)	9.609(1)	10.957(2)
b/Å	9.041(2)	17.220(6)	9.941(2)	15.503(3)
c/Å	16.202(5)	19.012(6)	12.612(2)	16.508(3)
α/°		71.79(2)	90.23(1)	108.64(2)
β/°	105.45(2)	84.00(3)	91.67(1)	106.91(2)
γ/°		86.36(3)	97.82(1)	92.72(2)
U/Å^3	2363.3(11)	2972(2)	1193.0(3)	2511.6(8)
Z	4	4	2	4
D_c/g cm^{-3}	2.364	1.980	2.243	2.173
F(000)	1600	1720	776	1584
μ(Mo-Kα)/cm^{-1}	20.10	15.80	19.61	18.68
Crystal dimensions/mm	0.38 × 0.58 × 0.38	0.5 × 0.5 × 0.3	0.3 × 0.4 × 0.3	0.4 × 0.5 × 0.5
Scan method	θ–2θ	Wyckoff ω	Wyckoff ω	θ–2θ
Total data	4585	11 158	4402	8501
Unique data	4150	10 460	4171	8045
Observed data, N_o	3442	10 457	4170	7092
Observation criterion $[F_o^2 > n\sigma(F_o^2)]$, *n*	2	−3	−3	2
Least-squares variables, N_v	352	922	384	716
*R*1	0.027[b]	0.026[c]	0.018[c]	0.022[b]
wR	0.037[b]	0.058[c]	0.041[c]	0.030[b]
g[b] (or *a*,*b*,*c*)[c]	0.0004	0.0218, 3.81, 30	0.013, 1.24, 40.0	0.0003
S	1.334[b]	1.106[c]	1.084[c]	1.29
Largest difference map peak (e Å^{-3})	+0.45	+0.72	+0.38	+0.49
Extinction correction			0.092(3)	0.001 16(4)

[a] Data common to all: $T = 295$ K; wavelength 0.710 73 Å, 2θ range 3–50°; [b] $R1 = \Sigma|\Delta|/\Sigma|F_o|$; $wR = (\Sigma w\Delta^2/\Sigma wF_o^2)^{\frac{1}{2}}$; $S = [\Sigma w\Delta^2/(N_o - N_v)]^{\frac{1}{2}}$, $\Delta = F_o - F_c$; $w = [\sigma_c^2(F_o) + gF_o^2]^{-1}$, $\sigma_c^2(F_o)$ = variance in F_o due to counting statistics. [c] $wR = (\Sigma w\Delta^2/\Sigma wF_o^4)^{\frac{1}{2}}$; $S = [\Sigma w\Delta^2/(N - N_v)]^{\frac{1}{2}}$; $R1 = \Sigma||F_o| - F_c||/\Sigma|F_o|$ for reflections with $F_o^2 > 2\sigma(F_o^2)$; $\Delta = F_o^2 - F_c^2$; $N = N_o$ + restraints; $w = [\sigma_c^2(F_o^2) + (aP)^2 + bP + c]^{-1}$, $\sigma_c^2(F_o^2)$ = variance in F_o^2 due to counting statistics, $P = [\max(F_o^2,0) + 2F_c^2]/3$.

Table 9 Atomic coordinates (× 10^4) for complex **3**

Atom	*x*	*y*	*z*	Atom	*x*	*y*	*z*
Ru(1)	7400(1)	1727(1)	6329(1)	F(9c)	5790(2)	−523(4)	5150(2)
Ru(2)	6789(1)	−487(1)	7118(1)	C(10)	8365(3)	−1090(6)	5294(3)
Ru(3)	8284(1)	642(1)	7864(1)	F(10a)	8315(2)	−266(4)	4596(2)
C(1)	6419(3)	2558(7)	5599(3)	F(10b)	7977(2)	−2359(4)	5016(2)
O(1)	5841(3)	3106(6)	5184(3)	F(10c)	9157(2)	−1458(4)	5594(2)
C(2)	7873(4)	3653(6)	6325(3)	C(11)	9352(3)	1077(6)	6598(3)
O(2)	8137(4)	4804(5)	6312(3)	F(11a)	9376(2)	1365(4)	5799(2)
C(3)	7907(3)	−1475(6)	7628(3)	F(11b)	9995(2)	183(4)	6938(2)
O(3)	8173(2)	−2670(4)	7775(2)	F(11c)	9537(2)	2368(4)	7016(2)
C(4)	7158(3)	1599(5)	7455(3)	C(21)	6260(5)	−2457(9)	7594(6)
C(5)	6765(4)	2807(7)	7852(3)	C(22)	5746(5)	−2135(12)	6768(5)
F(5a)	6637(3)	2432(4)	8614(2)	C(23)	5411(4)	−686(13)	6826(6)
F(5b)	6019(2)	3186(5)	7351(2)	C(24)	5665(4)	−195(9)	7644(5)
F(5c)	7219(2)	4041(4)	7983(2)	C(25)	6195(4)	−1238(10)	8124(4)
C(6)	7178(3)	−580(5)	6006(3)	C(31)	9230(5)	−237(8)	8998(4)
C(7)	8019(3)	−389(5)	5977(3)	C(32)	9580(3)	1014(10)	8654(4)
C(8)	8529(3)	451(5)	6677(3)	C(33)	9108(4)	2271(7)	8739(3)
C(9)	6539(4)	−1086(7)	5209(3)	C(34)	8506(4)	1823(7)	9135(3)
F(9a)	6715(2)	−680(4)	4465(2)	C(35)	8567(4)	296(7)	9281(3)
F(9b)	6449(2)	−2571(4)	5176(2)				

signal of **3** was first seen, at δ 5.41. On warming to room temperature complex **3** then gradually became the dominant species in solution. An attempt to isolate one or more of these intermediate species by carrying out a reaction of **2** with hexaflurobut-2-yne at −30 °C, followed by chromatography at the same temperature, was unsuccessful. However, the NMR data are consistent with the expected intermediacy of a complex of type **A** and in accord with the reaction of $CF_3C{\equiv}CCF_3$ following path (*b*)(*i*).

This work has revealed details of new pathways for alkyne linking and cleavage at a trinuclear metal centre, but the pathway followed by a particular alkyne is clearly very sensitive to the nature of its substituents.

Experimental

All reactions were carried out using dried and degassed solvents under a nitrogen atmosphere using standard Schlenk techniques. Column chromatography was carried out on alumina columns (*ca.* 3 × 30 cm). Infrared spectra were recorded on a Perkin-Elmer 1710 Fourier-transform spectrometer, using calcium fluoride cells of 1 mm path length, proton, ^{13}C and ^{19}F NMR spectra using JEOL FX-90, GX-270 and GX-400 spectrometers. Elemental analyses were performed by the Microanalytical Laboratory of the School of Chemistry. Fast atom bombardment mass spectra were carried out by the EPSRC Mass Spectrometry Service Centre at the University of

Table 10 Atomic coordinates (× 10^4) for complex **5**

Atom	*x*	*y*	*z*	Atom	*x*	*y*	*z*
Ru(1)	1 139(1)	3 416(1)	2 610(1)	Ru(1a)	2 979(1)	7 571(1)	2 413(1)
Ru(2)	−1 410(1)	4 064(1)	2 016(1)	Ru(2a)	3 466(1)	8 855(1)	2 984(1)
Ru(3)	−1 002(1)	4 127(1)	3 367(1)	Ru(3a)	2 329(1)	9 213(1)	1 690(1)
C(1)	2 459(4)	4 269(2)	2 284(2)	C(1a)	3 665(5)	6 475(2)	2 735(2)
O(1)	3 261(4)	4 769(2)	2 061(2)	O(1a)	4 057(4)	5 813(2)	2 941(2)
C(2)	2 498(4)	2 740(2)	2 278(2)	C(2a)	1 113(5)	7 201(3)	2 737(2)
O(2)	3 350(4)	2 340(2)	2 084(2)	O(2a)	6(4)	6 966(3)	2 925(2)
C(3)	374(4)	3 718(2)	1 529(2)	C(3a)	3 426(4)	7 621(2)	3 469(2)
O(3)	875(3)	3 716(2)	944(1)	O(3a)	3 525(5)	7 148(2)	4 051(2)
C(4)	−396(4)	4 883(2)	2 329(2)	C(4a)	1 453(4)	8 838(2)	2 778(2)
O(4)	123(3)	5 522(2)	2 051(2)	O(4a)	335(3)	8 764(2)	3 105(2)
C(5)	622(3)	3 305(2)	3 789(2)	C(5a)	2 767(3)	8 249(2)	1 241(2)
C(51)	1 530(3)	3 437(2)	4 334(2)	C(51a)	1 908(3)	8 105(2)	682(2)
C(52)	2 466(4)	4 069(3)	4 130(2)	C(52a)	615(4)	7 740(3)	873(2)
C(53)	3 316(5)	4 165(4)	4 640(4)	C(53a)	−119(5)	7 611(3)	330(3)
C(54)	3 260(5)	3 650(4)	5 351(4)	C(54a)	405(5)	7 847(3)	−401(3)
C(55)	2 301(6)	3 036(4)	5 572(3)	C(55a)	1 675(5)	8 223(3)	−604(2)
C(56)	1 435(5)	2 927(2)	5 072(2)	C(56a)	2 420(4)	8 348(2)	−68(2)
C(6)	551(3)	2 511(2)	3 703(2)	C(6a)	4 159(3)	7 896(2)	1 295(2)
C(61)	1 437(3)	1 796(2)	4 120(2)	C(61a)	4 710(3)	7 323(2)	870(2)
C(62)	2 892(4)	1 786(2)	4 052(2)	C(62a)	4 027(4)	6 618(2)	914(2)
C(63)	3 649(5)	1 156(3)	4 516(2)	C(63a)	4 484(5)	6 166(3)	431(2)
C(64)	2 971(5)	535(2)	5 061(2)	C(64a)	5 613(5)	6 411(3)	−86(2)
C(65)	1 527(5)	543(2)	5 142(2)	C(65a)	6 313(5)	7 096(3)	−123(2)
C(66)	754(4)	1 162(2)	4 670(2)	C(66a)	5 869(4)	7 549(2)	356(2)
C(7)	−422(3)	2 500(2)	3 178(2)	C(7a)	4 882(3)	8 154(2)	1 805(2)
C(9)	−493(4)	1 753(2)	2 931(2)	C(9a)	6 304(4)	7 769(3)	2 027(2)
F(1)	−1 317(3)	1 178(1)	3 408(1)	F(1a)	6 405(3)	6 959(2)	2 117(2)
F(2)	−1 005(3)	1 925(1)	2 266(1)	F(2a)	7 367(2)	8 097(2)	1 520(1)
F(3)	762(3)	1 370(1)	2 868(1)	F(3a)	6 611(2)	7 858(2)	2 672(1)
C(8)	−1 600(3)	3 146(2)	3 072(2)	C(8a)	4 404(3)	8 976(2)	1 897(2)
C(10)	−3 024(4)	2 799(3)	3 379(2)	C(10a)	5 431(4)	9 650(3)	1 529(2)
F(4)	−3 469(3)	2 291(2)	3 030(2)	F(4a)	6 698(3)	9 520(2)	1 802(2)
F(5)	−3 016(3)	2 329(2)	4 104(1)	F(5a)	5 698(3)	9 742(2)	793(1)
F(6)	−4 076(2)	3 355(2)	3 364(1)	F(6a)	4 998(3)	10 394(2)	1 571(2)
C(21)	−3 524(6)	4 608(6)	1 779(4)	C(21a)	4 716(7)	8 796(4)	3 930(3)
C(22)	−2 610(7)	5 142(4)	1 314(4)	C(22a)	3 293(7)	8 900(3)	4 160(2)
C(23)	−1 896(6)	4 765(4)	852(3)	C(23a)	2 792(8)	9 638(4)	3 712(3)
C(24)	−2 352(7)	3 956(5)	1 023(3)	C(24a)	3 893(9)	10 010(4)	3 204(3)
C(25)	−3 451(6)	3 877(4)	1 611(3)	C(25a)	5 107(7)	9 499(5)	3 348(3)
C(31)	−1 379(5)	4 272(3)	4 504(2)	C(31a)	1 753(8)	10 555(3)	1 445(3)
C(32)	−845(5)	5 016(3)	4 020(3)	C(32a)	516(8)	10 136(5)	1 621(3)
C(33)	−1 809(5)	5 355(3)	3 501(3)	C(33a)	423(6)	9 743(3)	1 081(4)
C(34)	−2 938(4)	4 826(3)	3 660(2)	C(34a)	1 621(6)	9 946(3)	587(2)
C(35)	−2 672(5)	4 162(3)	4 287(2)	C(35a)	2 376(6)	10 439(3)	815(3)

Table 11 Atomic coordinates (× 10^4) for complex **8**

Atom	*x*	*y*	*z*	Atom	*x*	*y*	*z*
Ru(1)	3477(1)	1633(1)	2080(1)	C(11)	5572(4)	2730(4)	4196(3)
Ru(2)	552(1)	1713(1)	2040(1)	C(12)	2709(3)	979(3)	4496(2)
Ru(3)	2292(1)	4050(1)	2058(1)	F(12a)	2836(3)	1458(2)	5497(1)
C(1)	4542(3)	212(3)	2369(2)	F(12b)	1465(2)	210(2)	4402(2)
O(1)	5212(3)	−624(2)	2529(2)	F(12c)	3668(2)	120(2)	4441(2)
C(2)	4174(3)	1673(3)	668(2)	C(13)	921(3)	3385(3)	4185(2)
O(2)	4626(3)	1675(3)	−148(2)	F(13a)	−188(2)	3980(2)	3857(2)
C(3)	1737(3)	150(3)	1818(2)	F(13b)	1790(2)	4344(2)	4729(2)
O(3)	1515(3)	−1002(2)	1626(2)	F(13c)	409(2)	2488(2)	4926(2)
C(4)	1480(3)	2769(3)	844(2)	C(21)	−1642(3)	2123(4)	2116(3)
O(4)	1451(2)	2779(2)	−87(2)	C(22)	−1516(3)	1496(4)	1128(3)
C(5)	4233(3)	3660(2)	2613(2)	C(23)	−1175(4)	202(4)	1324(3)
C(6)	4264(3)	2840(3)	3532(2)	C(24)	−1113(3)	29(4)	2448(3)
C(7)	2900(3)	2098(3)	3689(2)	C(25)	−1447(3)	1197(4)	2921(3)
C(8)	1673(3)	2782(2)	3304(2)	C(31)	3232(4)	6034(3)	1351(4)
C(9)	5553(3)	4484(3)	2247(2)	C(32)	1996(5)	5664(3)	804(3)
O(5)	5985(2)	5513(2)	2913(2)	C(33)	908(4)	5601(3)	1514(3)
O(6)	6147(2)	4280(2)	1456(2)	C(34)	1490(4)	5984(3)	2512(3)
C(10)	7207(4)	6425(4)	2599(3)	C(35)	2934(4)	6233(3)	2416(3)

Swansea. Trimethylamine *N*-oxide, dimethyl acetylenedicarboxylate, diphenylethyne, methyl but-2-ynoate, but-2-yne (Aldrich) and hexafluorobut-2-yne (Fluorochem) were used as supplied. Complex **1** was prepared by the method previously reported.[5]

Preparation of $[Ru_3(MeCN)(CO)_2(\mu\text{-}CO)(\mu_3\text{-}CO)\{\mu_3\text{-}C_2(CF_3)_2\}(\eta\text{-}C_5H_5)_2]$ **2**

To a dichloromethane solution (50 cm^3) of complex **1** (0.15 g, 0.20 mmol) was added trimethylamine *N*-oxide (Me_3NO)

Table 12 Atomic co-ordinates (× 10^4) for complex **12**

Atom	x	y	z	Atom	x	y	z
Ru(1)	2283(1)	3078(1)	3431(1)	Ru(1a)	−2936(1)	−1453(1)	3759(1)
Ru(2)	468(1)	2387(1)	1779(1)	Ru(2a)	−2340(1)	−1631(1)	2239(1)
Ru(3)	1798(1)	4700(1)	3217(1)	Ru(3a)	−5249(1)	−1209(1)	2751(1)
C(1)	1712(4)	1957(3)	3551(3)	C(1a)	−1732(4)	−2261(3)	3982(3)
O(1)	1370(4)	1295(2)	3629(2)	O(1a)	−1024(3)	−2752(3)	4106(3)
C(2)	2774(4)	3790(3)	4695(3)	C(2a)	−3987(4)	−1782(3)	4376(3)
O(2)	3056(4)	4192(3)	5440(2)	O(2a)	−4587(3)	−1996(3)	4762(2)
C(3)	3972(4)	2759(3)	3535(3)	C(3a)	−1853(4)	−477(3)	4811(3)
O(3)	4965(3)	2569(3)	3563(3)	O(3a)	−1202(3)	115(2)	5417(2)
C(4)	407(3)	3479(2)	3012(2)	C(4a)	−4029(3)	−2316(2)	2386(2)
C(8)	−545(4)	3450(3)	3506(3)	C(8a)	−4384(4)	−3344(3)	2128(3)
F(8a)	−1751(2)	3091(2)	2955(2)	F(8aa)	−4247(3)	−3833(2)	1352(2)
F(8b)	−625(3)	4285(2)	4049(2)	F(8ab)	−5612(3)	−3586(2)	2051(2)
F(8c)	−250(3)	2943(2)	4022(2)	F(8ac)	−3689(4)	−3659(2)	2736(2)
C(5)	65(3)	3799(2)	2236(2)	C(5a)	−4438(3)	−1887(2)	1695(2)
C(9)	−1146(4)	4193(3)	1885(3)	C(9a)	−5300(4)	−2344(3)	720(3)
F(9a)	−2108(2)	3558(2)	1286(2)	F(9aa)	−4680(3)	−2726(3)	168(2)
F(9b)	−1583(2)	4664(2)	2544(2)	F(9ab)	−6229(3)	−2977(2)	625(2)
F(9c)	−901(3)	4802(2)	1506(2)	F(9ac)	−5909(3)	−1730(2)	409(2)
C(6)	1097(3)	3757(2)	1815(2)	C(6a)	−3964(3)	−877(2)	2057(2)
C(10)	980(3)	3983(2)	978(2)	C(10a)	−4141(4)	−258(3)	1504(3)
O(4)	172(3)	3609(2)	261(2)	O(4a)	−3681(3)	−311(2)	922(2)
O(5)	1942(3)	4643(2)	1144(2)	O(5a)	−4848(3)	379(2)	1788(2)
C(12)	1991(6)	4883(4)	371(3)	C(12a)	−4969(7)	1083(4)	1375(4)
C(7)	2231(3)	3456(2)	297(2)	C(7a)	−3254(3)	−543(2)	3018(2)
C(11)	3311(3)	3384(2)	1899(3)	C(11a)	−2698(3)	456(2)	3419(2)
O(6)	3240(3)	2866(2)	1170(2)	O(6a)	−1979(3)	822(2)	3158(2)
O(7)	4371(2)	3959(2)	2480(2)	O(7a)	−3047(3)	897(2)	4131(2)
C(13)	5477(4)	3950(4)	2173(4)	C(13a)	−2477(5)	1858(3)	4609(3)
C(21)	−1292(4)	1481(3)	862(3)	C(21a)	−1578(4)	−2259(3)	1140(3)
C(22)	−443(6)	1553(3)	377(3)	C(22a)	−1191(4)	−1291(3)	1479(3)
C(23)	676(5)	1196(3)	724(3)	C(23a)	−422(4)	−1038(3)	2388(3)
C(24)	498(5)	913(3)	1415(3)	C(24a)	−331(4)	−1834(3)	2615(3)
C(25)	−715(4)	1097(3)	1498(3)	C(25a)	−1050(4)	−2594(3)	1848(3)
C(31)	1348(6)	6049(3)	3779(7)	C(31a)	−7338(4)	−1626(4)	2215(4)
C(32)	2159(7)	5827(3)	4463(4)	C(32a)	−6886(4)	−1614(3)	3105(3)
C(33)	3302(5)	5725(3)	4297(4)	C(33a)	−6322(4)	−706(3)	3676(3)
C(34)	3226(6)	5863(3)	3529(4)	C(34a)	−6411(5)	−164(3)	3122(4)
C(35)	2039(8)	6059(3)	3177(4)	C(35a)	−7035(4)	−735(4)	2220(4)

(0.023 g, 0.21 mmol) in acetonitrile (40 cm^3). Immediate darkening of the red solution occurred and IR spectroscopy showed the presence of **2**. Removal of solvent afforded a dark red solid which was used without further purification.

Reactions of complex 2

(*a*) **With hexafluorobut-2-yne.** Complex **2** (0.20 mmol) was prepared as described above and dissolved in CH_2Cl_2 (100 cm^3) in a Young's tube. The solution was frozen at −196 °C under vacuum and hexafluorobut-2-yne (0.07 g, 0.42 mmol) was condensed into the tube. The mixture was warmed to room temperature and stirred for 16 h, after which time the red solution had turned brown. Chromatography of the crude brown product revealed a single yellow-brown band, eluted with dichloromethane–hexane (1 : 4), which afforded a dark orange-brown solid $[Ru_3(CO)_2(\mu\text{-}CO)\{\mu_3\text{-}\eta^3\text{-}C_3(CF_3)_3\}(\mu_3\text{-}CCF_3)(\eta\text{-}C_5H_5)_2]$ **3** (0.075 g, 44%).

(*b*) **With hexafluorobut-2-yne at low temperature.** Complex **2** was prepared from **1** (0.025 g, 0.03 mmol) and Me_3NO (0.004 g, 0.04 mmol) and dissolved in CD_2Cl_2 (1 cm^3) in an NMR tube. The tube was evacuated, cooled to −196 °C, and hexafluorobut-2-yne (0.008 g, 0.05 mmol) was condensed in before sealing. The tube was then warmed to −95 °C (toluene–liquid N_2 slush bath) and a sequence of ^1H NMR spectra recorded between −90 °C and room temperature.

The reaction was repeated on a larger scale in a Young's tube (0.20 mmol of complex **2** with 0.42 mmol of hexafluorobut-2-yne) and the mixture allowed to react at −36 °C (1,2-dichloroethane–liquid N_2 slush bath) for 1 h. Column chromatography at −30 °C yielded one yellow band which afforded complex **3** (0.033 g, 19%) on elution with dichloromethane–hexane (1 : 4).

(*c*) **With diphenylethyne.** Complex **2** (0.20 mmol) was prepared as previously described and dissolved in CH_2Cl_2 (50 cm^3). Diphenylethyne (0.07 g, 0.39 mmol) was added and the mixture stirred for 20 h, over which time the dark red solution turned dark green. The crude product was chromatographed, yielding three bands. The first band (pink) was identified as *trans*-$[Ru_2(CO)\{\mu\text{-}C_4(CF_3)_2Ph_2\}(\eta\text{-}C_5H_5)_2]$ **4** (0.015 g, 11%), eluted with dichloromethane–hexane (1 : 9). The second band was red, eluted with dichloromethane–hexane (1 : 4), and afforded complex **1** (0.04 g, 27%). The third band was green, eluted with dichloromethane–hexane (1 : 1), and produced a green solid identified as $[Ru_3(CO)_2(\mu\text{-}CO)_2\{\mu_3\text{-}C_4(CF_3)_2Ph_2\}(\eta\text{-}C_5H_5)_2]$ **5** (0.051 g, 38%).

(*d*) **With methyl but-2-ynoate.** To a dichloromethane solution (50 cm^3) of complex **2**, prepared from **1** (0.20 g, 0.27 mmol) and Me_3NO (0.032 g, 0.29 mmol) in MeCN (50 cm^3), was added methyl but-2-ynoate (0.05 cm^3, 0.50 mmol). After stirring for 24 h the solution had darkened and removal of solvent revealed a brown solid. This gave five bands on a chromatography column: (*i*) pink, eluted with dichloromethane–hexane (1 : 9), afforded 0.02 g (10%) of **1**; (*ii*) red, eluted with dichloromethane–hexane (1 : 4), produced red crystalline *trans*-$[Ru_2(CO)\{\mu\text{-}C_4(CF_3)_2Me(CO_2Me)\}(\eta\text{-}C_5H_5)_2]$ **6** (0.017 g, 10%); (*iii*) yellow, eluted with dichloromethane–hexane (1 : 4), yielded 0.022 g (13%) of yellow crystalline *cis*-$[Ru_2(CO)\{\mu\text{-}C_4(CF_3)_2Me(CO_2Me)\}(\eta\text{-}C_5H_5)_2]$ **7**; (*iv*) green, eluted with dichloromethane–hexane (1:1), afforded a dark green solid identified as $[Ru_3(CO)_2(\mu\text{-}CO)_2\{\mu_3\text{-}C_4(CF_3)_2Me(CO_2Me)\}(\eta\text{-}C_5H_5)_2]$ **8** (0.034 g, 15%); and (*v*) yellow, afforded a small amount of an unidentified yellow solid after elution with dichloromethane–hexane (2:3).

(*e*) **With but-2-yne.** Complex **2**, prepared from **1** (0.12 g, 0.16 mmol) and Me_3NO (0.018 g, 0.16 mmol) as described previously, was dissolved in CH_2Cl_2 (50 cm^3). But-2-yne (0.03 cm^3, 0.38 mmol) was added at 0 °C and the mixture stirred at 0–20 °C for 16 h, over which time it darkened. Removal of solvent followed by chromatography gave two bands. The first band (red) eluted with dichloromethane–hexane (1:4) and yielded 0.031 g (17%) of **1**. Further elution with dichloromethane–hexane (3:7) gave a green band which afforded the green solid $[Ru_3(CO)_2(\mu\text{-}CO)_2\{\mu_3\text{-}C_4(CF_3)_2Me_2\}(\eta\text{-}C_5H_5)_2]$ **9** (0.02 g, 22%).

(*f*) **With dimethyl acetylenedicarboxylate.** Complex **2** was prepared as described above (0.20 mmol) and dissolved in CH_2Cl_2 (50 cm^3). To this was added dmad (0.05 cm^3, 0.41 mmol) and the mixture stirred for 0.5 h, during which time it darkened. Removal of solvent yielded an oily dark red residue, which when chromatographed produced five bands: (*i*) red, eluted with dichloromethane–hexane (1:5), afforded 0.021 g (14%) of $[Ru_3(CO)_3(\mu\text{-}CO)(\mu_3\text{-}CO)\{\mu_3\text{-}C_2(CF_3)_2\}(\eta\text{-}C_5H_5)_2]$ **1**; (*ii*) pink, eluted with dichloromethane–hexane (2:3), produced 0.057 g (42%) of the pink solid *trans*-$[Ru_2(CO)\{\mu\text{-}C_4(CF_3)_2(CO_2Me)_2\}(\eta\text{-}C_5H_5)_2]$ **10**; (*iii*) yellow, eluted with dichloromethane–hexane (1:1), yielded 0.020 g (11%) of the yellow crystalline solid $[Ru_3(CO)_5\{C_2(CF_3)_2\}\{C_2(CO_2Me)_2\}(\eta\text{-}C_5H_5)_2]$ **11**; (*iv*) and (*v*), red and green respectively, which were unidentified.

Reactions of complex 1

(*a*) **With dimethyl acetylenedicarboxylate.** A toluene solution (100 cm^3) of complex **1** (0.100 g, 0.14 mmol) was heated at reflux with dmad (0.03 cm^3, 0.24 mmol) for 3 h, resulting in a change from red to dark brown. The solvent was removed and the solid brown residue chromatographed, affording three bands: (*i*) yellow, eluted with dichloromethane–hexane (3:7), yielded 0.025 g (22%) of the yellow crystalline solid $[Ru_3(CO)_3\{\mu_3\text{-}C_4(CF_3)_2(CO_2Me)_2\}(\eta\text{-}C_5H_5)_2]$ **12**; (*ii*) pink, eluted with dichloromethane–hexane (2:3), afforded 0.023 g (25%) of *trans*-$[Ru_2(CO)\{\mu\text{-}C_4(CF_3)_2(CO_2Me)_2\}(\eta\text{-}C_5H_5)_2]$ **10**; (*iii*) yellow, eluted with dichloromethane–hexane (1:1), produced 0.021 g (18%) of $[Ru_3(CO)_5\{C_2(CF_3)_2\}\{C_2(CO_2Me)_2\}(\eta\text{-}C_5H_5)_2]$ **11**.

(*b*) **With methyl but-2-ynoate.** A toluene solution (120 cm^3) of complex **1** (0.12 g, 0.16 mmol) and of methyl but-2-ynoate (0.02 cm^3, 0.20 mmol) was refluxed for 2.5 h, after which time the red solution had turned brown. Chromatography of the crude product revealed three bands: (*i*) yellow, eluted with dichloromethane–hexane (3:17), produced a yellow solid identified as $[Ru_3(CO)_3\{\mu_3\text{-}C_4(CF_3)_2Me(CO_2Me)\}(\eta\text{-}C_5H_5)_2]$ **13** (0.022 g, 17%); (*ii*) red, eluted with dichloromethane–hexane (1:4), afforded *trans*-$[Ru_2(CO)\{\mu\text{-}C_4(CF_3)_2Me(CO_2Me)\}(\eta\text{-}C_5H_5)_2]$ **6** (0.012 g, 12%); (*iii*) yellow, eluted with dichloromethane–hexane (1:4) afforded 0.01 g (10%) of *cis*-$[Ru_2(CO)\{\mu\text{-}C_4(CF_3)_2Me(CO_2Me)\}(\eta\text{-}C_5H_5)_2]$ **7**.

(*c*) **With diphenylethyne.** Diphenylethyne (0.096 g, 0.54 mmol) and complex **1** (0.20 g, 0.27 mmol) were dissolved in toluene (100 cm^3) and refluxed for 1.5 h. A gradual change from red to dark orange occurred. Removal of solvent under reduced pressure produced a dark orange crude product which exhibited two main bands when introduced to a chromatography column: (*i*) orange, eluted with dichloromethane–hexane (1:9), afforded an orange crystalline solid (0.103 g, 44%), identified as a mixture of the isomers $[Ru_3(CO)_3\{\mu_3\text{-}C_4(CF_3)_2Ph_2\}(\eta\text{-}C_5H_5)_2]$ **14a** and $[Ru_3(CO)_3\{\mu_3\text{-}C_4(CF_3)Ph_2(CF_3)\}(\eta\text{-}C_5H_5)_2]$ **14b**; (*ii*) pink, eluted with dichloromethane–hexane (1:9), produced 0.027 g (14%) of the pink solid *trans*-$[Ru_2(CO)\{\mu\text{-}C_4(CF_3)Ph_2(CF_3)\}(\eta\text{-}C_5H_5)_2]$ **15**. A third green band was also visible on the column, but this was not identified.

(*d*) **With but-2-yne.** To a toluene solution (100 cm^3) of complex **1** (0.12 g, 0.16 mmol), but-2-yne (0.02 cm^3, 0.26 mmol) was added. The mixture was refluxed for 3 h, over which time the red solution turned orange-brown. Removal of solvent, followed by chromatography, gave three main products: (*i*) yellow, eluted with hexane, produced a yellow solid, identified as $[Ru_3(CO)_3\{\mu_3\text{-}C_4(CF_3)_2Me_2\}(\eta\text{-}C_5H_5)_2]$ **16a** (0.02 g, 17%); (*ii*) orange, eluted with hexane, which on removal of solvent gave an orange solid characterised as $[Ru_3(CO)_3\{\mu_3\text{-}C_4(CF_3)Me_2(CF_3)\}(\eta\text{-}C_5H_5)_2]$ **16b** (0.054 g, 46%); (*iii*) brown, eluted with dichloromethane–hexane (1:4), afforded the orange-brown solid $[Ru_3(CO)_2(\mu\text{-}CO)\{\mu_3\text{-}\eta^3\text{-}C_3(CF_3)Me_2\}(\mu_3\text{-}CCF_3)(\eta\text{-}C_5H_5)_2]$ **17** (0.028 g, 24%).

(*e*) **With hexafluorobut-2-yne.** A toluene solution (70 cm^3) of complex **1** (0.125 g, 0.17 mmol) in an evacuated Carius tube was frozen at −196 °C. Hexafluorobut-2-yne (0.11 g, 0.68 mmol) was condensed in and the tube sealed. Heating at 100 °C for 4 h caused a change from red to red-brown. Evaporation of solvent followed by chromatography produced one band, eluted with dichloromethane–hexane (1:4), identified as complex **3** (0.07 g, 49%).

Heating of complexes

$[Ru_3(CO)_2(\mu\text{-}CO)_2\{\mu_3\text{-}C_4(CF_3)_2Ph_2\}(\eta\text{-}C_5H_5)_2]$ 5. A toluene solution (80 cm^3) of complex **5** (0.07 g, 0.08 mmol) was refluxed for 1 h, after which time the green solution had turned dark orange. Removal of solvent followed by chromatography yielded an orange band which afforded 0.03 g (45%) of $[Ru_3(CO)_3\{\mu_3\text{-}C_4(CF_3)Ph_2(CF_3)\}(\eta\text{-}C_5H_5)_2]$ **14b**, eluted with dichloromethane–hexane (1:9). A very small amount (*ca.* 0.002 g, 4%) of *trans*-$[Ru_2(CO)\{\mu\text{-}C_4(CF_3)Ph_2(CF_3)\}(\eta\text{-}C_5H_5)_2]$ **15** was also isolated.

$[Ru_3(CO)_2(\mu\text{-}CO)_2\{\mu_3\text{-}C_4(CF_3)_2Me(CO_2Me)\}(\eta\text{-}C_5H_5)_2]$ 8. A toluene solution (50 cm^3) of complex **8** (0.01 g, 0.01 mmol) was refluxed for 0.5 h. The green solution turned orange and IR spectroscopy revealed the presence of only $[Ru_3(CO)_3\{\mu_3\text{-}C_4(CF_3)_2Me(CO_2Me)\}(\eta\text{-}C_5H_5)_2]$ **13** and *trans*-$[Ru_2(CO)\{\mu\text{-}C_4(CF_3)_2Me(CO_2Me)\}(\eta\text{-}C_5H_5)_2]$ **6**.

$[Ru_3(CO)_2(\mu\text{-}CO)_2\{\mu_3\text{-}C_4(CF_3)_2Me_2\}(\eta\text{-}C_5H_5)_2]$ 9. A toluene solution (50 cm^3) of complex **9** was refluxed for 0.5 h. The solution changed from green to orange and IR spectroscopy revealed the presence of only $[Ru_3(CO)_3\{\mu_3\text{-}C_4(CF_3)Me_2(CF_3)\}(\eta\text{-}C_5H_5)_2]$ **16b** and $[Ru_3(CO)_2(\mu\text{-}CO)\{\mu_3\text{-}\eta^3\text{-}C_3(CF_3)Me_2\}(\mu_3\text{-}CCF_3)(\eta\text{-}C_5H_5)_2]$ **17**.

Structure determinations for complexes 3, 5, 8 and 12

Many of the details of the structure analyses carried out on complexes **3**, **5**, **8** and **12** are listed in Table 8. X-Ray diffraction measurements were made at room temperature using Siemens four-circle R3m/V diffractometers on single crystals mounted in thin-walled glass capillaries. Cell dimensions for each analysis were determined from the setting angle values of 20–30 centred reflections. For each structure analysis intensity data were collected for unique portions of reciprocal space and corrected for Lorentz, polarisation and long-term intensity fluctuations on the basis of the intensities of check reflections repeatedly measured during data collection. Corrections for X-ray absorption effects were applied on the basis of azimuthal scan data. The structures were solved by heavy-atom (Patterson and Fourier difference) methods, and refined by least squares against F (**3** and **12**) or F^2 (**5** and **8**). In each of **5** and **12** there are two crystallographically distinct molecules of complex present. All non-hydrogen atoms were assigned anisotropic displacement parameters and refined without positional constraints. All hydrogen atoms were constrained to ideal geometries except in the case **5** and **8** for which all hydrogens other than H(22), H(25) and H(25a) for **5** and H(10a)–H(10f) for **8** were refined without positional constraints. All hydrogen atoms were assigned isotropic displacement parameters. Isotropic extinction corrections were applied in the cases of **8** for which $F_c = F_c^{\text{uncorr.}}/(1 + 0.001xF_c^2\lambda^3/\sin 2\theta)^{\frac{1}{4}}$ and **12** for which $F_c = F_c^{\text{uncorr.}}/[1 + (0.002xF_c^2/\sin 2\theta)]^{\frac{1}{4}}$, where the refined parameter values x are given in Table 8.

Final difference syntheses showed no chemically significant features, the largest being close to the metal. Refinements converged smoothly to residuals given in Table 8. Tables 9–12 report the positional parameters. All calculations were made with programs of the SHELXTL PLUS and SHELXL packages.[15] Complex neutral-atom scattering factors were taken from ref. 16.

Complete atomic coordinates, thermal parameters and bond lengths and angles have been deposited at the Cambridge Crystallographic Data Centre. See Instructions for Authors, *J. Chem. Soc., Dalton Trans.*, 1996, Issue 1.

Acknowledgements

We are grateful to the SERC for the award of research studentships (to K. J. A. and J. J. B.) and support, and Johnson Matthey plc for a loan of ruthenium trichloride.

References

1 S. A. R. Knox, R. F. D. Stansfield, F. G. A. Stone, M. J. Winter and P. Woodward, *J. Chem. Soc., Dalton Trans.*, 1982, 173.
2 L. A. Brady, A. F. Dyke, S. E. Garner, V. Guerchais, S. A. R. Knox, J. P. Maher, S. M. Nicholls and A. G. Orpen, *J. Chem. Soc., Chem. Commun.*, 1992, 4.
3 L. A. Brady, A. F. Dyke, S. E. Garner, S. A. R. Knox, A. Irving, S. M. Nicholls and A. G. Orpen, *J. Chem. Soc., Dalton Trans.*, 1993, 487.
4 S. A. R. Knox, B. R. Lloyd, D. A. V. Morton, A. G. Orpen and M. L. Turner, *Polyhedron*, 1995, **14**, 2723.
5 K. J. Adams, J. J. Barker, J. P. H. Charmant, C. Ganter, G. Klatt, S. A. R. Knox, A. G. Orpen and S. Ruile, *J. Chem. Soc., Dalton Trans.*, 1994, 477.
6 E. Sappa, *J. Cluster Sci.*, 1994, **5**, 211 and refs. therein.
7 A. D. Clauss, J. R. Shapley, C. N. Wilker and R. Hoffmann, *Organometallics*, 1984, **3**, 619.
8 J. A. Hriljac and D. F. Shriver, *J. Am. Chem. Soc.*, 1987, **109**, 6010.
9 Y. Chi and J. R. Shapley, *Organometallics*, 1985, **4**, 1900.
10 R. Rumin, F. Robin, F. Y. Pétillon, K. W. Muir and I. Stevenson, *Organometallics*, 1991, **10**, 2274.
11 S. M. Nicholls, Ph. D. Thesis, University of Bristol, 1991.
12 A. R. Kudinov, M. I. Rybinskaya, Y. T. Struchkov, A. I. Yanovskii and P. V. Petrovskii, *J. Organomet. Chem.*, 1987, **336**, 187.
13 M. I. Rubinskaya and A. R. Kudinov, *Organomet. Chem. USSR*, 1989, **2**, 12.
14 J. W. Lauher, M. Elian, R. H. Summerville and R. Hoffmann, *J. Am. Chem. Soc.*, 1976, **98**, 3219.
15 G. M. Sheldrick, SHELXTL PLUS, Revision 4.2, University of Göttingen, 1990; SHELXL 93, University of Göttingen, 1993.
16 *International Tables for Crystallography*, Kluwer, Dordrecht, 1992, vol. C; *International Tables for X-Ray Crystallography*, Kynoch Press, Birmingham, 1974, vol. 4.

Received 7th August 1995; *Paper* 5/05280G